ALMA MATER STUDIORUM · UNIVERSITÀ DI BOLOGNA

Scuola di Scienze
Corso di Laurea Magistrale in Fisica

A two-body study of dynamical expansion in the XXZ spin chain and equivalent interacting fermion model

Relatore:
Prof.ssa Elisa Ercolessi

Presentata da:
Claudio D'Elia

Correlatore:
Dott. Piero Naldesi

Sessione II
Anno Accademico 2013/2014

"Do not read so much, look about you and think of what you see there."
R.P. Feynman
[letter to Ashok Arora, 4 January 1967, published in Perfectly Reasonable
Deviations from the Beaten Track (2005) p. 230]

Abstract

Lo scopo di questa tesi è studiare l'espansione dinamica di due fermioni interagenti in una catena unidimensionale cercando di definire il ruolo degli stati legati durante l'evoluzione temporale del sistema.

Lo studio di questo modello viene effettuato a livello analitico tramite la tecnica del Bethe ansatz, che ci fornisce autovalori ed autovettori dell'hamiltoniana, e se ne valutano le proprietà statiche. Particolare attenzione è stata dedicata alle caratteristiche dello spettro al variare dell'interazione tra le due particelle e alle caratteristiche degli autostati. Dalla risoluzione dell'equazione di Bethe vengono ricercate le soluzioni che danno luogo a stati legati delle due particelle e se ne valuta lo spettro energetico in funzione del momento del centro di massa. Si è studiato inoltre l'andamento del numero delle soluzioni, in particolare delle soluzioni che danno luogo ad uno stato legato, al variare della lunghezza della catena e del parametro di interazione.

La valutazione delle proprietà dinamiche del modello è stata effettuata tramite l'utilizzo dell'algoritmo t-DMRG (time dependent - Density Matrix Renormalization Group). Questo metodo numerico, che si basa sulla decimazione dello spazio di Hilbert, ci permette di avere accesso a quantità che caratterizzano la dinamica quali la densità e la velocità di espansione. Da queste sono stati estratti i profili dinamici della densità e della velocità di espansione al variare del valore del parametro di interazione .

Contents

List of Figures

List of Tables

Chapter 1

Introduction

A poet once said, 'The whole universe is in a glass of wine.' We will probably never know in what sense he meant it, for poets do not write to be understood. But it is true that if we look at a glass of wine closely enough we see the entire universe. There are the things of physics: the twisting liquid which evaporates depending on the wind and weather, the reflection in the glass; and our imagination adds atoms. The glass is a distillation of the earth's rocks, and in its composition we see the secrets of the universe's age, and the evolution of stars. What strange array of chemicals are in the wine? How did they come to be? There are the ferments, the enzymes, the substrates, and the products. There in wine is found the great generalization; all life is fermentation. Nobody can discover the chemistry of wine without discovering, as did Louis Pasteur, the cause of much disease. How vivid is the claret, pressing its existence into the consciousness that watches it! If our small minds, for some convenience, divide this glass of wine, this universe, into parts – physics, biology, geology, astronomy, psychology, and so on – remember that nature does not know it! So let us put it all back together, not forgetting ultimately what it is for. Let it give us one more final pleasure; drink it and forget it all! [8]

Since ancient times man has always tried to give an explanation for natural phenomena. From thunders to fire passing throught the gravity, every single event has always stimulated the intellect of our ancestors so that they could explain in a more-or-less logic way the causes and the mechanics of that event.
With the upcoming of the scientific method, they started to fix the groundwork of modern science: the study of natural phenomena must be performed with reproducible experiments and the results must have universal validity.
From here begins the study and the understading of the mechanics of celestial bodies, universal gravitation, electromagnetic waves propagation and this let the world be as we know it today.
Doubtless, this wouldn't been possible if in the meantime they didn't de-

velop a very powerful tool which is mathematics. This shortly become the common language of scientists which, over the century, enriched its "lexicon" with algebra, calculus, complex analysis, differential geometry, etc...
However, at the dawn of XX century, something imperilled further scientific development. An unimmaginable limit was reached, scientists started to investigate the micro-universe of the elementary consituent of matter.
With all the difficulties that could arise, an handful of men were able to cross the enemy lines and to understand the encryption key of this microscopic enigma.
Quantum mechanics was taking its first steps.

Even if its understanding weren't within everyone's means, quantum mechanics is the perfect equipment for the scientist who wants to explore the unknown terrain of the microscopic matter. He will be going to deal with something that he probably can only imagine.
Here arise a new problem, what are the limits of applicability of this new theory?
In principle quantum mechanics can be applied to almost all the problem which involve particles, atoms, molecules, etc... Its limit are of practical nature.

Let us consider now to have at our disposal 50 g of pure iron. These are made up by about 10^{23} atoms and every atom is made up by 26 electrons and as many protons and neutrons inside nucleus. Besides, electrons and protons have an electrical charge, so they will interact mutually. Thus, trying to describe the electronic motion in a conductor, we're going to deal with an overwhelming number of interactions between particles and this give rise to a many body problem which is nearly impossible to solve.

Nevertheless, there is a way to go. If we quit "something" it is possible to describe an alternative problem which still has the same properties or at least the most interesting of the original one.
For example, we could imagine that the atoms of a conductor are arranged on a regular lattice with a fixed interspace within atoms and that the electrons are faster than the nuclei so that we can assume the nuclei fixed at their lattice positions. Moreover, taking account of the screening effect of the electrons in an atom, we can assume that the ionic potential is felt only from electrons on the same atom or from electrons on the nearest neighbours.
With all these "reasonable" assumptions we can reduce the initial problem to a simpler one but on the other hand it still preserve all the key features of the original.

So, we've shaped what is called a model!

In last century many electronic and magnetic models has been developed. The study of these models has provided results more and more accurate and close to the experimental results.

The simplest electronic model of a conductor is the free electron gas. In this model we don't take account of the interacting potential due to the presence of the underlying cristalline structure and we consider only the valence electrons which are confined in the conductor.
Despite the extreme exemplification, Sommerfeld in 1927 managed to obtain a good theorical prediction for the electrical conductivity, the temperature dependence of the electronic specific heat and the mean free path of electrons.
From this starting point one can refine the model making it closer to reality. Considering that the ions are fixed to their lattice positions and they possess an electric charge, one could introduce a periodic potential into the model.
That was done by Bloch in 1928, his theorem ensures that a solution to this problem can exist and, moreover, the resolution of the model via the Bloch functions has revealed the existence of the energy bands.

Proceeding one could arrive to what is the state of art of electronic models, or rather, the Hubbard[12] model and all of its "derivates".

The Hubbard model is of great relevance in the modern theoretical physics, in fact many theorists[20][7][1] have devoted a considerable part of their careers to the Hubbard model.
Altought it is the simplest many-particle model one can write down, it cannot be reduced to a single-particle theory.
The ground state is known to be complicated (i.e., a superposition of many Fock states). In most cases its analytic form is unknown, except in one dimension.
The Bethe ansatz is one of the methods that can be used to resolve the 1D Hubbard model[11]. Results in two or three dimensions are not yet known.

In an analogous way we can follow the evolution of the models developed to explain the magnetic phenomena of the matter.

The starting point for the study of the magnetic properties has been the study of the molecule of hydrogen. In fact, this brought to recognize the effects of the exchange interaction (independently W.Heisenberg and P.Dirac

in 1926) which is a direct effect of the spin property of electrons.

Among other consequences, the exchange interaction is responsible for ferromagnetism and of the volume of matter. It has no classical analogue.

The Heisenberg hamiltonian, for a system of two electrons, is:

$$H^{Heis} = -2J(\widehat{s}_1 \cdot \widehat{s}_2) \tag{1.1}$$

where J is the exchange integral and $\widehat{s}_1$, $\widehat{s}_2$ are the spin operators of the two electrons.

Generalizing this hamiltonian to a chain of spins one can obtain the XXX spin chain model which describes the magnetic systems taking account of the interaction between the magnetic momenta of the electrons which lies on nearest neighbour atoms.

At a first sight it might seem an oversimplified model, instead it can predict accurately the magnetic properties of some metals.

The most general case in the XYZ model, it considers that the value of the exchange integral can be dependent on the axis along which the magnetic interaction takes place.

This mean to consider the internal anisotropy of the materials.

One step behind in complexity but not in interest, we find the XXZ model which considers the anisotropy only along the z-direction.

Although this could appear a more simplistic model, it actually is of great practical importance in the physics of magnetic materials. In fact, the need of mass memory devices more and more capacious, has been fulfilled thanks to the properties of "perpendicular anisotropy" of some layered materials[6][13].

The XXZ Model describes a spin chain with next-neighbour interaction, anisotropy on the z-axis and an external applied magnetic field along the z-axis.

The spin at each site is described in terms of the operators S^x, S^y and S^z. These operators must satisfy to the right commutation relations for spin $\frac{1}{2}$ particles

$$[S_i^\alpha, S_j^\beta] = -i\delta_{i,j}\epsilon_{\alpha\beta\gamma}S_i^\gamma \tag{1.2}$$

One possibility is to define S operators via the Pauli matrices σ^x, σ^y, σ^z:

$-\infty < \Delta \leq -1$	Antiferromagnetic	$\Delta = -1$ XXX AFM Model
$-1 < \Delta < 1$	Paramagnetic	$\Delta = 0$ XY Model
$1 \leq \Delta < \infty$	Ferromagnetic	$\Delta = 1$ XXX FM Model

Table 1.1: Variety of magnetic behaviours described by the XXZ model varying Δ.

$$
\begin{aligned}
S^x &= \frac{1}{2}\sigma^x = \frac{1}{2}\begin{pmatrix} 0 & 1 \\ 1 & 0 \end{pmatrix} \\
S^y &= \frac{1}{2}\sigma^y = \frac{1}{2}\begin{pmatrix} 0 & -i \\ i & 0 \end{pmatrix} \\
S^z &= \frac{1}{2}\sigma^z = \frac{1}{2}\begin{pmatrix} 1 & 0 \\ 0 & -1 \end{pmatrix}
\end{aligned}
$$

The interaction terms are of the kind $S_i^\alpha S_{i+1}^\alpha$ where $\alpha = x, y, z$, so the Hamiltonian of the system for a chain of lenght L is

$$
H = -J\sum_{i=1}^{L}(S_i^x S_{i+1}^x + S_i^y S_{i+1}^y + \Delta S_i^z S_{i+1}^z) + h\sum_{i=1}^{L} S_i^z \qquad (1.3)
$$

where J is the strenght of the interaction and $J > 0$, Δ is the anisotropy parameter and h is the external applied field.

Varying the value of Δ in this Hamiltonian, one can describe a wide range of magnetic behaviours as show in the following table

This model has been investigated by many authors[30],[31],[32],[33],[3],Orbach[21]and Walker[26] generalized the Bethe ansatz method for $\Delta \neq 1$ in order to resolve that model.
Analytical results of this model are known also when a magnetic field along the z-direction is applied

The subject of this thesis will be the 1D spinless fermions chain which is a direct descendant of the Hubbard model.

The spinless fermion model is a particular case of the Hubbard model.
In the spinless fermion model (from here SF model) only singular site occupations are possible, so the interaction is considered between adjacent sites.
Thereby, considering a 1D chain of lenght L, the Hamiltonian for this model

is:

$$H = -\frac{t}{2}\sum_{i=1}^{L}(c_{i+1}^{+}c_{i} + c_{i}^{+}c_{i+1}) + U\sum_{i=1}^{L}n_{i}n_{i+1} - (U-\mu)\sum_{i=1}^{L}n_{i} + \frac{(U-2\mu)}{4} \quad (1.4)$$

Where t is the hopping parameter, U the strenght of the interaction and μ is the chemical potential.

In the following we will see that the 1D SF model is equivalent to the XXZ $\frac{1}{2}$ spin chain model by mean of the Jordan-Wigner transformation.

1.1 Recent development in the study of interacting systems

In last few years condensed matter physics gained an incredible input from the simulation of quantum systems via cold atoms trapped into optical lattices.
It is possible to load ultra-cold atoms into an optical lattice in order to perform an experimental "real-time" simulation of a bosonic of fermionic system. The ability to control various system parameters in real time has not only allowed quantum simulations of equilibrium properties of interacting many-body systems, but has also enabled experimental studies of quantum quenches and particle transport in clean, well-controlled, and isolated systems.

As example we could consider the experiment of Kinoshita, Weiss and Wenger[16], they prepared a quantum 1D bose gas into an optical lattice using ultracold atoms of ^{87}Rb.
An array of 1D bose gases is obtained from a Bose-Einstein condensate loaded into a 2D optical lattice with tight transverse confinement.
At t=0 the atoms are trapped with an anharmonic potential into a superposition of states with opposite momentum, at later times this anharmonic potential is removed and atoms starts their evolution traveling along the 1D chain.
Kinoshita, Weiss and Wenger observed that after a long time (27 ms which are equivalent to thousand of collisions) the system does not show any sign of equilibrium.
Their conclusions are related to the problem of finding a relation between the integrability and the thermalization of a system. As they conclude in

their paper[16], these "results are probably explainable by the well-known fact that a homogeneous 1D Bose gas with point-like collisional interactions is integrable".

So, cold atoms trapped in optical lattices open the way to a broad variety of experiments which could conferm theorical predictions or, on the other hand, the experimental results could be the starting spark of a theoretical work aimed to explain these results.

As already said, in this work we will study two strongly interacting models, the SF chain model and the spin $\frac{1}{2}$ XXZ model.
It is well known that the models we choose can be mapped one into another by means of a Jordan-Wigner transformation. So all of our results can be straightforwardly translated from spins to particles and it is possible to make predictions over a wide range of 1D models: Luttinger liquid, Hubbard with a nearest-neighbor density-density attractive or repulsive interaction, FM, AFM or paramagnet.

In chapter 2 we will apply the Coordinate Bethe Ansatz (CBA) method to these models and obtain the exact eigenfunctions for the two body case (two particles for the SF model two down-spins for the XXZ model). Moreover, we show explicitily that the two considered models can be translated one into the other by means of the Jordan-Wigner transformation and we calculate the termodynamic limit prediction for the energy.
In chapter 3 the solutions of the Bethe equation are analyzed, we will see that the value of the interaction parameter plays a key role in determining the eigenfunctions and the ground state. Moreover, we will see that solving numerically the Bethe equation one needs particular care when dealing with an even value of the chain lenght L, in this case, in fact, there are some numerical issues which could bring to the loss of solutions.
In chapter 4 we give an outlook on other works which deal with the time evolution of an interacting system and there are some general comments on the time evolution of a system.
In chapter 5 there is a general review about the DMRG technique used to simulate numerically the time evolution of this system after a quantum quench of the interacting parameter. Quenching the interaction parameter i.e. to change suddenly its value, this allows to study the evolution of the system which starts from a condition of non-equilibrium.We will investigate the expansion dynamics of the two particles SF model starting from a chain in

which a large chemical potential bind the particles in the middle sites of the chain, the system is then "released" removing the chemical potential and activating the interaction parameter U.

In the end results from time evolution are shown for various values of U ranging from $-4 \leq U \leq 4$. We will evaluate the density profile during the expansion finding that the group spreading velocitiy is strongly influenced by the value of the interaction parameter U.

Chapter 2

Coordinate Bethe ansatz and Bethe equations

In 1931, Hans Bethe[2] presented a method, which is nowadays called the "Coordinate Bethe ansatz" (CBA), for calculating the exact eigenvalues and eigenvectors of the one-dimensional spin $\frac{1}{2}$ XXX Heisenberg model.

The term "Bethe ansatz", refers to the wave function Bethe had used for the eigenvectors. Since then, many other quantum many body systems have been solved by some variant of the Bethe ansatz. One problem especially worth mentioning is the repulsive interaction quantum gas problem which has been solved by C. N. Yang in the late sixties[34],[9]. For this he used the Bethe ansatz twice; the second time in a generalized form which is often called the "Bethe-Yang" ansatz. Following this result, the repulsive interaction problem with an arbitrary irreducible representation of the permutation group was solved by B. Sutherland by repeated use of the Bethe-Yang ansatz[24].

The Bethe ansatz in some variant of its original formulation is now used to solve many other 1D quantum many body systems.

The Bethe ansatz is an exact method for the calculation of eigenvalues and eigenvectors of a certain class of quantum many-body model systems. Also if the eigenvalues and eigenvectors for a finite system may be obtained with other methods, as for example a brute force numerical diagonalization, the Bethe ansatz offers two important advantages:

1. all eigenstates are characterized by a set of quantum numbers which can be used to distinguish them according to specific physical properties;

2. in many cases the eigenvalues and the physical properties derived from them can be evaluated in the thermodynamic limit.

2.1 Coordinate Bethe Ansatz on Spinless Fermion Chain

In this thesis this method is going to be applied to two particular models: the XXZ spin chain and the Spinless Fermions chain.
Let us consider first the Hamiltonian of a 1D spinless fermion chain:

$$H^{SF} = -\frac{t}{2} \sum_{i=1}^{L} \left(c_i^+ c_{i+1} + c_{i+1}^+ c_i \right) + U \sum_{i=1}^{L} (n_i - \frac{1}{2})(n_{i+1} - \frac{1}{2}) + \mu \sum_{i=1}^{L} (n_i - \frac{1}{2})$$

$$(2.1)$$

where t is the hopping parameter, U is the interaction strenght and μ the chemical potential.
The operators c_i^+ and c_i are the creation and annihilation operators for the femionic particles. These operators can be applied to Fock's state e.g. the vacuum $|0\rangle$, their effect is to change the occupation number of a given site:

$$c_i^+|0\rangle = |i\rangle \qquad c_i|i\rangle = |0\rangle \qquad c_i|0\rangle = 0 \qquad c_i^+|i\rangle = 0 \qquad (2.2)$$

These operators act on fermionic states, so their anti-commutation rules are:

$$\left\{ c_i^+, c_j \right\} = \delta_{i,j} \qquad \left\{ c_i, c_j \right\} = 0 \qquad \left\{ c_i^+, c_j^+ \right\} = 0 \qquad (2.3)$$

The hamiltonian commutes with the number operator n_i, this gives in turn that the total number of particles is a conserved quantity.
Thus we can block diagonalize this hamiltonian defining the number of particles r. Applying the Bethe ansatz for every value of $r = 0, 1, 2, \ldots, L$ we can obtain the exact eigenvectors and eigenvalues.

For $r = 0$ it is almost trivial: the eigenvector is the fermionic vacuum $|0\rangle$ and its eigenvalue is

$$E_0 = \frac{UL}{4} - \frac{\mu L}{2}. \qquad (2.4)$$

For $r = 1$ there is only one particle in the chain and we have to consider eigenvectors of the form:

$$|\phi^{(1)}\rangle = \sum_{j=1}^{L} \phi_j c_j^+ |0\rangle \tag{2.5}$$

here ϕ_j is the single particle wave function.
We can use a plane wave for the ansatz:

$$\phi_j = A e^{ijp} \tag{2.6}$$

From the normalization we get that the coefficient $A = \frac{1}{\sqrt{L}}$.
The energy resulting from the Schroedinger equation will be:

$$E = -t \cos(p) + (\mu - U) + E_0 \tag{2.7}$$

We want to study the model under periodic boundary conditions.
Our chain is defined to start from 1 so applying PBC means to require that the site $L + 1$ is equivalent to the site 1.
So:

$$\phi_1 = \frac{1}{\sqrt{L}} e^{ip} = \frac{1}{\sqrt{L}} e^{iLp} e^{ip} = \phi_{L+1} \tag{2.8}$$

This position gives us a quantization rule for the momentum of the particle:

$$p = \frac{2\pi n}{L} \tag{2.9}$$

where n is an integer from 0 to $L - 1$.
This complete the study for the case $r = 1$.

2.1.1 Coordinate Bethe ansatz for the spinless fermion chain when r=2

Now we concentrate our study to the case of 2 particles on a chain of lenght L.
It's quite different from the previous we just considered, but it is the key to

understand how to work out the Bethe ansatz in the general case when $r \geq 2$.

Applying the Bethe ansatz, we request that eigenvectors are of the form:

$$|\phi^{(2)}\rangle = \sum_{j,k=1}^{L} \phi_{j,k} c_j^+ c_k^+ |0\rangle \qquad (2.10)$$

with $\phi_{j,k}$ defined in the following way:

$$\phi_{j,k} = [Ae^{i(p_1 j + p_2 k)} + Be^{i(p_1 k + p_2 j)}]\theta(j-k) - [Ae^{i(p_1 k + p_2 j)} + Be^{i(p_1 j + p_2 k)}]\theta(k-j) \qquad (2.11)$$

Here p_1 and p_2 are the momenta of the particles, j and k their coordinates.
A and B are two coefficients, in the most general case they are c-number.
Pauli's exclusion principle and wave function antisimmetry are automatically implemented in this ansatz.
Applying the hamiltonian to $|\phi^{(2)}\rangle$ one gets:

$$\sum_{j=1}^{L}\sum_{k=1}^{L}[-\frac{t}{2}(\phi_{j+1,k} + \phi_{j,k+1} + \phi_{j-1,k} + \phi_{j,k-1})+$$

$$+\phi_{j,k}(U\delta_{j,k+1} + U\delta_{k,j+1} - 2U + 2\mu + \frac{UL}{4} - \frac{\mu L}{2} - E)]|j,k\rangle = 0 \qquad (2.12)$$

Where the energy takes the free form:

$$E = -2t\left(\cos(p_1) + \cos(p_2)\right) + 2(\mu - U) + E_0 \qquad (2.13)$$

Considering eq. (12) when $j - k = 1$ - or equivalently $j - k = -1$- and substituting the expression for the energy, we obtain a condition for the amplitude ratio:

$$\frac{A}{B} = -\frac{1 + e^{i(p_1 + p_2)} + \frac{2U}{t}e^{ip_1}}{1 + e^{i(p_1 + p_2)} + \frac{2U}{t}e^{ip_2}} \qquad (2.14)$$

Eq.(2.14) is called Bethe equation.
Furthermore, it can be shown that the quantity $\frac{A}{B}$ is equivalent to a phase, so:

$$\frac{A}{B} = e^{i\theta} \qquad (2.15)$$

The details of the derivation of the Bethe equation are in Appendix 1.

2.1.2   Boundary condition and quantization rules for r=2

We remember that our chain is defined to start from 1 so applying PBC means to require that the site $L + 1$ is equivalent to the site 1.
In terms of the Bethe ansatz, for two particles, this is achieved with the position:

$$
\begin{aligned}
\phi_{j,k} &= \phi_{k,j+L} \\
&\Downarrow \\
[Ae^{i(p_1 j + p_2 k)} + Be^{i(p_1 k + p_2 j)}] &= [Ae^{i(p_1 k + p_2 j)}e^{ip_2 L} + Be^{i(p_1 j + p_2 k)}e^{ip_1 L}]
\end{aligned}
\tag{2.16}
$$

whenever $p_1 \neq p_2$, with some algebra and considering that $e^{i(p_1 j + p_2 k)}$ and $e^{i(p_1 k + p_2 j)}$ are linearly independent vectors, we obtain the following equation for the quantities p_1 and p_2:

$$
\frac{A}{B} = e^{ip_1 L} \tag{2.17a}
$$

$$
\frac{B}{A} = e^{ip_2 L} \tag{2.17b}
$$

with:

$$
p_1 = \frac{2\pi\lambda_1}{L} + \frac{\theta}{L} \tag{2.18a}
$$

$$
p_2 = \frac{2\pi\lambda_2}{L} - \frac{\theta}{L} \tag{2.18b}
$$

λ_1 and λ_2 are integers from 0 to $L - 1$ and they are called Bethe quantum number.

Considering $\theta = \alpha + i\beta$ and the relations obtained from the PBC, eq. (2.17a) can be rewritten as:

$$
-\frac{1 + e^{i\left(\frac{2\pi(\lambda_1 + \lambda_2)}{L}\right)} + \frac{2U}{t}e^{-\frac{\beta}{L}}e^{i\left(\frac{2\pi\lambda_1 + \alpha}{L}\right)}}{1 + e^{i\left(\frac{2\pi(\lambda_1 + \lambda_2)}{L}\right)} + \frac{2U}{t}e^{\frac{\beta}{L}}e^{i\left(\frac{2\pi\lambda_2 - \alpha}{L}\right)}} = e^{i\alpha}e^{-\beta} \tag{2.19}
$$

Varying the value of λ_1 and λ_2 one can solve this equation and find all the allowed value for α and β - subsequently for θ and so for p_1 and p_2.
What we are going to see in next chapter is that the solutions are strongly correlated to the value of U.

Considering that we are dealing with 2 particles, it could be useful to use the center of mass coordinates. So we can define:

$$X = \frac{j+k}{2} \qquad x = j - k \qquad P = p_1 + p_2 \qquad p = \frac{p_1 - p_2}{2} \qquad (2.20)$$

The ansatz takes the form:

$$\phi_{j,k} = sgn(x)e^{iPX}[Ae^{ip|x|} + Be^{-ip|x|}] \qquad (2.21)$$

The Bethe equation and PBC become:

$$-\frac{1 + e^{iP} + \frac{2U}{t}e^{i(\frac{P}{2}+p)}}{1 + e^{iP} + \frac{2U}{t}e^{i(\frac{P}{2}-p)}} = (-1)^{(\lambda_1+\lambda_2)}e^{-ipL} \qquad (2.22)$$

$$p = \frac{\pi(\lambda_1 - \lambda_2)}{L} + \frac{\theta}{L} \qquad (2.23a)$$

$$P = \frac{2\pi(\lambda_1 + \lambda_2)}{L} \qquad (2.23b)$$

2.1.3   Coordinate Bethe ansatz for $r > 2$

The 1D SF chain and the 1D XXZ spin chain belongs to the class of integrable models.
Integrable, or equivalently exactly solvable, models are very important in physics. Their importance is due both to theoretical points of view and experimental ones, because in such cases theoretical results and experimental results can be compared without ambiguity.
In condensed matter theory, the fundamental problem is that of solving many-body interacting systems and it is quite rare to encounter exactly solvable cases.
In fact, to solve the N body problem is an almost simple task for $N = 2$, but in most cases it could became not soluble for $N \geq 3$.

However, considering one dimensional systems, there are some solvable models. The SF model and the spin $\frac{1}{2}$ XXZ chain are examples of solvable models for a generic value of N.

In these cases we can write down many-body eigenfunctions using the method of the Bethe-ansatz. In this environment the N-body wave function is represented as a linear combination of $N!$ plane waves with N quasi-momenta. Many people focused their studies on the spin $\frac{1}{2}$ XXZ chain, Orbach in [21] and Walker in [26] have applied Bethe ansatz method to the case $\Delta \neq 1$, Yang and Yang in [30]-[33] worked out a fully investigation of the ground state of this model, Bonner and Fisher in [3] studied this model using the exact diagonalization method up to N = 12.

The study of the spin $\frac{1}{2}$ XXZ chain with $N > 2$ with a generic value of Δ has been done by Takahashi in [25].

Here we apply the results of Takahashi for the spin $\frac{1}{2}$ XXZ chain with $M > 2$ translating them in the language and the notation of the SF model with $r > 2$.

In this case the eigenstate is written as:

$$|\phi^{(r)}\rangle = \sum_{j_1,j_2\cdots j_r=1}^{L} \phi_{j_1,j_2\cdots j_r} c_{j_1}^+ c_{j_2}^+ \cdots c_{j_r}^+ |0\rangle \qquad (2.24)$$

Note that the notation is slightly different from the one used in eq. (2.10) but the meaning is unchanged.

In this case the wave function $\phi_{j_1,j_2\cdots j_r}$ is defined as:

$$\phi_{j_1,j_2\cdots j_r} = \sum_{Q}^{r!} A(Q)\exp(i\sum_{k=1}^{r} p_{Qk}j_k) \qquad (2.25)$$

As in the previous case the p's are the momenta and the j's are the position on the chain. $A(Q)$'s are the coefficients (just as A and B in the case $r = 2$), Q is a permutation of the indeces k $1, 2, \ldots, r$:

$$Q = \begin{pmatrix} 1 & 2 & \cdots & r \\ Q1 & Q2 & \cdots & Qr \end{pmatrix} \qquad (2.26)$$

The energy is again the sum of single particle's energy, so:

$$E = -t\sum_{j=1}^{r} \cos(p_j) + (\mu - U)r + E_0 \qquad (2.27)$$

The periodic boundary conditions set the equation:

$$(-1)^{r-1} \prod_{l \neq k} \frac{1 + e^{i(p_l+p_k)} + \frac{2U}{t}e^{ip_k}}{1 + e^{i(p_l+p_k)} + \frac{2U}{t}e^{ip_l}} = e^{ip_k L} \qquad (2.28)$$

Solving this equation will give us the allowed value for momenta of all particles, from these value we can write explicitly eigenvectors and their eigenvalues.

2.1.4 Thermodynamic limit

Recalling eqs.(2.22),(2.23a),(2.23b) we have the following system:

$$A(1 + e^{iP} + \frac{2U}{t}e^{iP/2}e^{ip}) + B(1 + e^{iP} + \frac{2U}{t}e^{iP/2}e^{-ip}) = 0 \qquad (2.29a)$$

$$\frac{A}{B} = -e^{iPL/2}e^{ipL} \qquad (2.29b)$$

$$P = \frac{2\pi n}{L} \qquad (2.29c)$$

with some substitutions:

$$\frac{A}{B}(1 + e^{i\frac{2\pi n}{L}} + \frac{2U}{t}e^{i\frac{\pi n}{L}}e^{ip}) + (1 + e^{i\frac{2\pi n}{L}} + \frac{2U}{t}e^{i\frac{\pi n}{L}}e^{-ip}) = 0 \qquad (2.30a)$$

$$\frac{A}{B} = -e^{i\pi n}e^{ipL} \qquad (2.30b)$$

So, from eqs. (2.30a) and (2.30b), requesting that $p = i\alpha$:

$$-e^{i\pi n}e^{-\alpha L}(1 + e^{i\frac{2\pi n}{L}} + \frac{2U}{t}e^{i\frac{\pi n}{L}}e^{-\alpha})+$$

$$+(1 + e^{i\frac{2\pi n}{L}} + \frac{2U}{t}e^{i\frac{\pi n}{L}}e^{\alpha}) = 0 \qquad (2.31a)$$

$$\frac{A}{B} = -e^{i\pi n}e^{-\alpha L} \qquad (2.31b)$$

In the TD limit $L \to \infty$ these eqs. gives:

$$1 + e^{iP} + \frac{2U}{t} e^{i\frac{P}{2}} e^{\alpha} = 0 \tag{2.32a}$$

$$\frac{A}{B} = 0 \tag{2.32b}$$

where $P \in [0, 2\pi]$.

Resolving the 1st order equation:

$$2\cos(\frac{P}{2}) + \frac{2U}{t} e^{\alpha} = 0 \tag{2.33}$$

$$\alpha^{TD} = \ln\left(-\frac{t\cos(\frac{P}{2})}{U}\right) \tag{2.34}$$

Thus, we have a prediction for the energy of a bound state in the thermodynamic limit:

$$E_P^{TD} = -2t\cos(\frac{P}{2})\cos\left(i\ln\left(-\frac{t\cos(\frac{P}{2})}{U}\right)\right) \tag{2.35}$$

or in a more simple form:

$$E_P^{TD} = \frac{t^2\cos^2(\frac{P}{2})}{U} + tU \tag{2.36}$$

2.2 Coordinate Bethe ansatz on XXZ Spin chain

The Hamiltonian of the XXZ model on a L-lenght spin chain is:

$$H^{XXZ} = -\frac{J}{2}\sum_{i=1}^{L}\left(S_i^x S_{i+1}^x + S_i^y S_{i+1}^y\right) - J\Delta\sum_{i=1}^{L} S_i^z S_{i+1}^z - h\sum_{i=1}^{L} S_i^z \tag{2.37}$$

Here J is the hopping parameter, Δ is the anisotropy strenght and h is the

external applied field.

The operators S_i^x, S_i^y and S_i^z are spin operators, their definition is based on the Pauli's matrices:

$$S_i^x = \frac{1}{2}\sigma^x \qquad S_i^y = \frac{1}{2}\sigma^y \qquad S_i^z = \frac{1}{2}\sigma^z \qquad (2.38)$$

The commutation rules for these operators are:

$$\left[S_i^\alpha, S_j^\beta\right] = i\delta_{i,j}\epsilon_{\alpha,\beta,\gamma}S_i^\gamma \qquad \text{with } \alpha, \beta, \gamma = x, y, z \qquad (2.39)$$

In absence of external applied field the ground state for this hamiltonian can be either a chain with every spin pointing the "down" direction or a chain with every spin pointing the "up" direction.
The presence of the external field break the degeneracy. From here we will consider $h > 0$ so the ground state will be a chain of "up" pointing spin, we can represent this state in this way:

$$|\Psi^{GS}\rangle = |\uparrow\uparrow \cdots \uparrow\uparrow\rangle \qquad (2.40)$$

The energy E_0 of the ground state is:

$$E_0 = -\frac{J\Delta L}{4} - \frac{hL}{2} \qquad (2.41)$$

For the sake of clarity hereafter we will denote the Fock states for this model with the same notation used for the spinless fermion chain. So the ground state will be noted as $|0\rangle$ and the state in which there is a rotated spin, for example in the i-th site, will be written as $|i\rangle$.
The XXZ model has the major property to conserve the total magnetization along the z-axis, $S_{TOT}^z = \sum_{j=1}^L S_j^z$. So the maximum magnetization is when all spins are oriented in the same direction and its value is $S_{MAX}^z = \frac{N}{2}$.

Considering that $\left[H^{XXZ}, S_{TOT}^z\right] = 0$ so the Hilbert space can be divided into sector with a given magnetization. This give us the possibility to study the model with a fixed number (M) of rotated spins.

A further simplification of the work cames from the possibility to define two operators which act by rotating spin in a given site. These operators are

defined as follow:

$$S_i^+ = \frac{S_i^x + iS_i^y}{2} \qquad S_i^- = \frac{S_i^x - iS_i^y}{2} \tag{2.42}$$

They are called respectively raising and lowering operators, in fact they act on the states in the following way:

$$S_i^+|0\rangle = |i\rangle S_i^+|i\rangle = 0 \qquad S_i^-|0\rangle = 0 S_i^-|i\rangle = |0\rangle \tag{2.43}$$

Rewriting the hamiltonian with these new operators we obtain:

$$\widetilde{H}^{XXZ} = -\frac{J}{2}\sum_{i=1}^{L}\left(S_i^+ S_{i+1}^- + S_{i+1}^+ S_i^-\right) - J\Delta\sum_{i=1}^{L} S_i^z S_{i+1}^z - h\sum_{i=1}^{L} S_i^z \tag{2.44}$$

The derivation of the Bethe equations for the spin $\frac{1}{2}$ XXZ Spin chain model is analogous to the spinless fermion model.
To keep contact with the spinless fermion model, we will consider the case in which there are two down pointing spins in the chain, so $M = 2$. Following the Bethe ansatz prescription the eigenstates of this hamiltonian must be of the form:

$$|\phi\rangle = \sum_{j,k=1}^{L} \phi_{j,k} S_j^- S_k^- |0\rangle \tag{2.45}$$

$\phi_{j,k}$ is defined in the same way of eq. (2.11):

$$\phi_{j,k} = [Ae^{i(p_1 j + p_2 k)} + Be^{i(p_1 k + p_2 j)}]\theta(j-k) - [Ae^{i(p_1 k + p_2 j)} + Be^{i(p_1 j + p_2 k)}]\theta(k-j) \tag{2.46}$$

As in the case of the spinless fermion p_1 and p_2 are the momenta of the particles, j and k their coordinates. A and B are two coefficients, in the most general case they are c-number.

Again, we can use the center of mass coordinates to describe the problem (as defined in eq. (2.20)).
What is slightly different from the previous case is the expression for the energy, in this case we have:

$$E = E_0 + J\left(\Delta - 2\cos(\frac{P}{2})\cos(p)\right) + h \tag{2.47}$$

But the equation for the amplitude ratio still have the same form of eq. (2.14):

$$\frac{A}{B} = -\frac{1 + e^{i(p_1+p_2)} - 2\Delta e^{ip_2}}{1 + e^{i(p_1+p_2)} - 2\Delta e^{ip_1}} \qquad (2.48)$$

The only difference is the coefficient -2Δ instead of $\frac{2U}{t}$.

What remain to do is to impose the periodic boundary conditions. It is easy to see that we would obtain the same Bethe equation of the spinless fermion model.
Imposing PBC will give us exactly eqs. (2.17a) and (2.17b), what is different in this case is the amplitude ratio that we just obtained.
So the equation to be solved for the spin $\frac{1}{2}$ XXZ spin chain model is:

$$-\frac{1 + e^{i(p_1+p_2)} - 2\Delta e^{ip_2}}{1 + e^{i(p_1+p_2)} - 2\Delta e^{ip_1}} = e^{ip_1 L} \qquad (2.49a)$$

The analogy with the spinless fermion model is evident.

2.3 Equivalence of two models: Jordan-Wigner transformation

The Jordan-Wigner transformation[14] (hereafter JWT) allow us to switch between the SF and the XXZ model.

The JWT are defined as:

$$c_i = e^{-i\pi \sum_{j=1}^{i-1} S_j^+ S_j^-} S_i^+ \qquad (2.50)$$

$$c_i^+ = S_i^- e^{i\pi \sum_{j=1}^{i-1} S_j^+ S_j^-} \qquad (2.51)$$

The operators $S_k^\pm$ satisfy to locally anti-commutation fermionic rules but when defined on different sites they commute:

$$\{S_j^+, S_j^-\} = 1$$
$$[S_j^+, S_k^-] = 0$$

The term $e^{-i\pi \sum_{j=1}^{i-1} S_j^- S_j^+}$ gives to the fermionic operators c_i^+ and c_i a global anti-commutation property which is what needed.

The transformations can be inverted to:

$$S_i^+ = e^{i\pi \sum_{j=1}^{i-1} c_j^+ c_j} c_i \qquad (2.52)$$

$$S_i^- = c_i^+ e^{-i\pi \sum_{j=1}^{i-1} c_j^+ c_j} \qquad (2.53)$$

It can be easily verified that $c_j^+ c_j = S_j^+ S_j^-$.

As last tool let us see that

$$S_k^+ S_k^- = S_k^x S_k^x + i(S_k^y S_k^x - S_k^x S_k^y) + S_k^y S_k^y \qquad (2.54)$$

So considering that

$$\left[S_i^\alpha, S_j^\beta \right] = i\delta_{i,j}\epsilon_{\alpha,\beta,\gamma} S_i^\gamma \qquad \text{with } \alpha, \beta, \gamma = x, y, z \qquad (2.55)$$

we can write

$$S_k^z = S_k^+ S_k^- - \frac{1}{2} \qquad (2.56)$$

Consider now the spin $\frac{1}{2}$ XXZ model hamiltonian defined with the raising and lowering operators:

$$\widetilde{H}^{XXZ} = -\frac{J}{2} \sum_{i=1}^{L} \left(S_i^+ S_{i+1}^- + S_{i+1}^+ S_i^- \right) - J\Delta \sum_{i=1}^{L} S_i^z S_{i+1}^z - h \sum_{i=1}^{L} S_i^z \quad (2.57)$$

Note that the PBC's are an important feature to be considered. In fact, let us consider what happen applying the JWT to the term $\sum_{i=1}^{L} S_i^+ S_{i+1}^-$:

$$\begin{aligned}
\sum_{i=1}^{L} S_i^+ S_{i+1}^- &= e^{i\pi \sum_{j=1}^{i-1} c_j^+ c_j} c_i c_{i+1}^+ e^{-i\pi \sum_{j=1}^{i} c_j^+ c_j} = \\
&= \sum_{i=1}^{L} e^{-i\pi c_i^+ c_i} c_i c_{i+1}^+ = \\
&= \sum_{i=1}^{L-1} e^{-i\pi c_i^+ c_i} c_i c_{i+1}^+ + e^{-i\pi c_L^+ c_L} c_L c_{L+1}^+ \qquad (2.58)
\end{aligned}$$

Now, $e^{-i\pi c_i^+ c_i}$ can be written as:

$$
\begin{aligned}
e^{-i\pi c_i^+ c_i} &= \sum_{j=0}^{\infty} \frac{\left(-i\pi c_i^+ c_i\right)^j}{j!} = \\
&= \sum_{j=1}^{\infty} \frac{(-i\pi)^j}{j!} c_i^+ c_i + 1 = \\
&= \left[\left(-1 + \sum_{j=1}^{\infty} \frac{(-i\pi)^j}{j!} \right) c_i^+ c_i + 1 \right] = \\
&= \left[(-1 + \cos(\pi) + i\sin(\pi)) c_i^+ c_i + 1 \right] = \\
&= 1 - 2 c_i^+ c_i
\end{aligned}
$$

So the term for $i = L$ in eq. (2.58) is not well-defined since it would be $(1 - 2c_L^+ c_L) c_L c_{L+1}^+$ and the $L+1$-th site isn't in the chain.
However, considering the PBC, the $L+1$-th site will coincide with the first site and, from eq. (2.58):

$$
\begin{aligned}
&= \sum_{i=1}^{L-1} (1 - 2c_i^+ c_i) c_i c_{i+1}^+ + (1 - 2c_L^+ c_L) c_L c_1^+ = \\
&= \sum_{i=1}^{L} (1 - 2c_i^+ c_i) c_i c_{i+1}^+ = \sum_{i=1}^{L} c_i c_{i+1}^+
\end{aligned}
$$

Applying the JWT to the entire hamiltonian one gets in a some straightforward way to:

$$
\widetilde{H}^{XXZ} = -\frac{J}{2} \sum_{i=1}^{L} \left(c_i^+ c_{i+1} + c_{i+1}^+ c_i \right) - J\Delta \sum_{i=1}^{L} n_i n_{i+1} + J\Delta \sum_{i=1}^{L} n_i - h \sum_{i=1}^{L} n_i - \frac{J\Delta L}{4} + \frac{hL}{2}
\tag{2.59}
$$

which have to be confronted with the hamiltonian of the Spinless Fermion model:

$$
H^{SF} = -\frac{t}{2} \sum_{i=1}^{L} \left(c_i^+ c_{i+1} + c_{i+1}^+ c_i \right) + U \sum_{i=1}^{L} n_i n_{i+1} - U \sum_{i=1}^{L} n_i + \mu \sum_{i=1}^{L} n_i + \frac{UL}{4} - \frac{\mu L}{2}
\tag{2.60}
$$

The corrispondence between the coefficient is evident:

$$
\begin{aligned}
J &= t \\
U &= -J\Delta = -t\Delta \\
\mu &= -h
\end{aligned}
$$

With these relations on mind we can verify that the Bethe equation obtained for the SF model can be switched directly into the one obtained for the XXZ model simply substituting $U = -J\Delta$.

Chapter 3

Results from Bethe equation

In the following we will discuss the solutions of the Bethe equation when $r = 2$ for the SF model and $M = 2$ for the XXZ model.

Since the only difference between eq. (2.14) and (2.48) is given by the coefficient $\frac{2U}{t}$ or $-\Delta$, we can solve one of them and take the solution for both. Let us consider eq. (2.19) and rewrite it in the following way:

$$-\frac{2\cos\left(\frac{\pi}{L}(\lambda_1 + \lambda_2)\right) + \frac{2U}{t}e^{-\frac{\beta}{L}}e^{i\frac{\pi(\lambda_1 - \lambda_2) + \alpha}{L}}}{2\cos\left(\frac{\pi}{L}(\lambda_1 + \lambda_2)\right) + \frac{2U}{t}e^{\frac{\beta}{L}}e^{-i\frac{\pi(\lambda_1 - \lambda_2) + \alpha}{L}}} = e^{-\beta}e^{i(2\pi\lambda_1 + \alpha)} \qquad (3.1)$$

Fixing the values of L and U and requiring that

$$
\begin{aligned}
-\pi &\leq \alpha \leq \pi \quad \text{if} \quad \beta \neq 0 \\
-\pi &< \alpha < \pi \quad \text{if} \quad \beta = 0
\end{aligned}
\qquad (3.2)
$$

this equation gives one solution for every possible choose of the couple λ_1, λ_2. There are L possible values for λ_1 and λ_2 so the solutions are L^2.

Anyway, all the solutions for which λ_1 and λ_2 are exchanged results to be dependent solutions. So, in order to obtain only the $\frac{L(L-1)}{2}$ independent solutions, we must require that $0 \leq \lambda_2 \leq \lambda_1 \leq L - 1$.

Also with this requirement one must be very carefull to do not take dependent solutions of the kind $\theta_{\lambda_1,\lambda_2} = -\theta_{\lambda_1,\lambda_2}$. Moreover when $\lambda_1 = \lambda_2$ the solution $\theta = 0$ must be eliminated cause it would give $p_1 = p_2$, as already said in this case $e^{i(p_1 j + p_2 k)}$ and $e^{i(p_1 k + p_2 j)}$ do not represent a set of independent vectors and the PBC fails.

As done by Karbach and Muller[15] studying the Heisenberg model, the eq. (3.1) can be solved numerically, it could be convenient to classify the couples (λ_1, λ_2) into three classes:

1. Class C1 - couples with $\lambda_2 = 0$ and $\lambda_1 = 0, 1, \ldots, L - 1$

2. Class C2 - couples with $\lambda_1 - \lambda_2 \geq 2$ but $\lambda_1, \lambda_2 \neq 0$

3. Class C3 - couples with $\lambda_1 = \lambda_2$ or $\lambda_1 = \lambda_2 + 1$ but $\lambda_1, \lambda_2 \neq 0$

Following this scheme, together with the prescription $0 \leq \lambda_2 \leq \lambda_1 \leq L-1$, we have L couples of class C1, $\frac{L}{2}(L - 5) + 3$ couples of class C2 and $2L - 3$ couples of class C3.
One could expect that every single couple yields a solution, but summing the number of C1, C2 and C3 couples we obtain a total number of $\frac{L}{2}(L + 1)$ couples.
So not every couple (λ_1, λ_2) can produce a solution.
Actually, there are some "missed" solutions for some values of λ_1 and λ_2, it depends strongly on the value of U and L.

In figs (3.1,3.2,3.3,3.4), are shown the solutions for every couple (λ_1, λ_2). It turns out that all the C2 couples produces always a solutions (light blue circles), so we have at least $\frac{L}{2}(L-5)+3$ solutions and they are always scattering solutions. The solutions from C1 and C3 couples , instead, can produce either scattering (blue squares for C3 and green squares for C1) or bound state (red squares for C3 and black stars for C1) solutions.
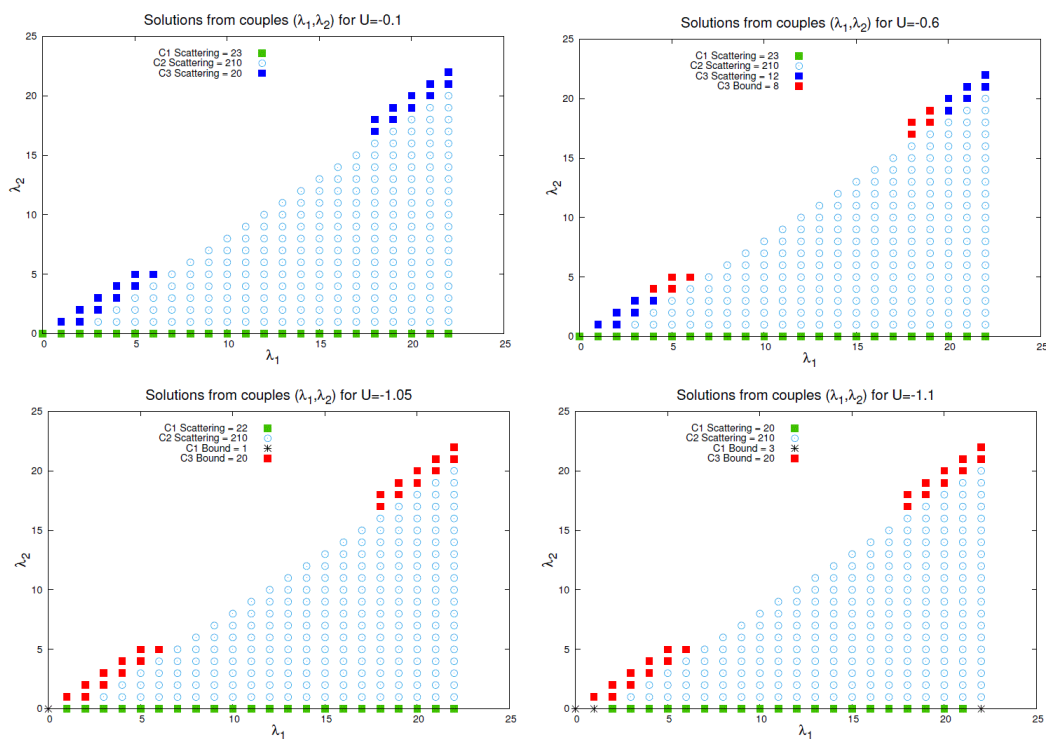
Figure 3.1: Couples of (λ_1, λ_2) for which there is a solution to the Bethe equation for $L = 23$ and $U < 0$.
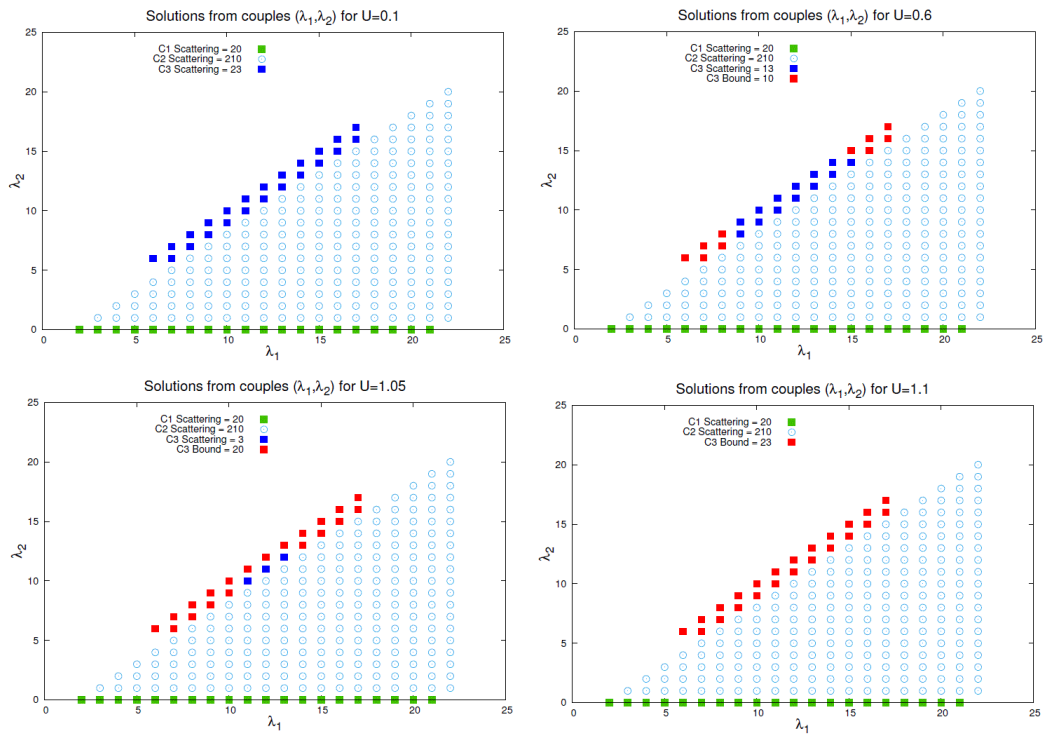
Figure 3.2: Couples of (λ_1, λ_2) for which there is a solution to the Bethe equation for $L = 23$ and $U > 0$.
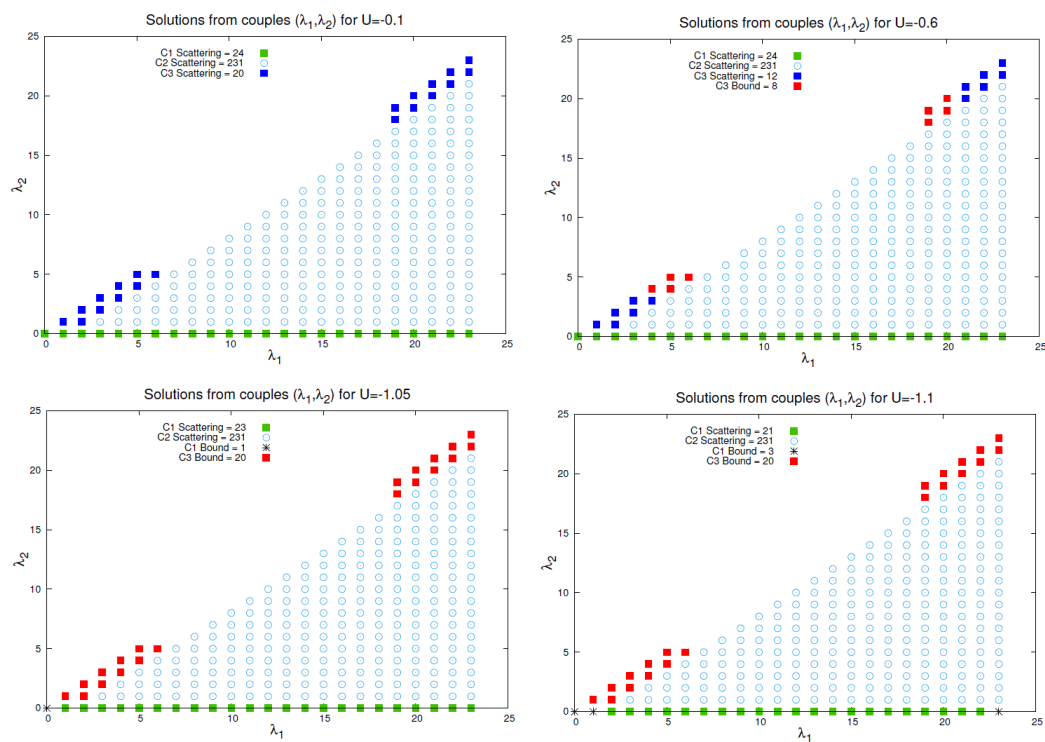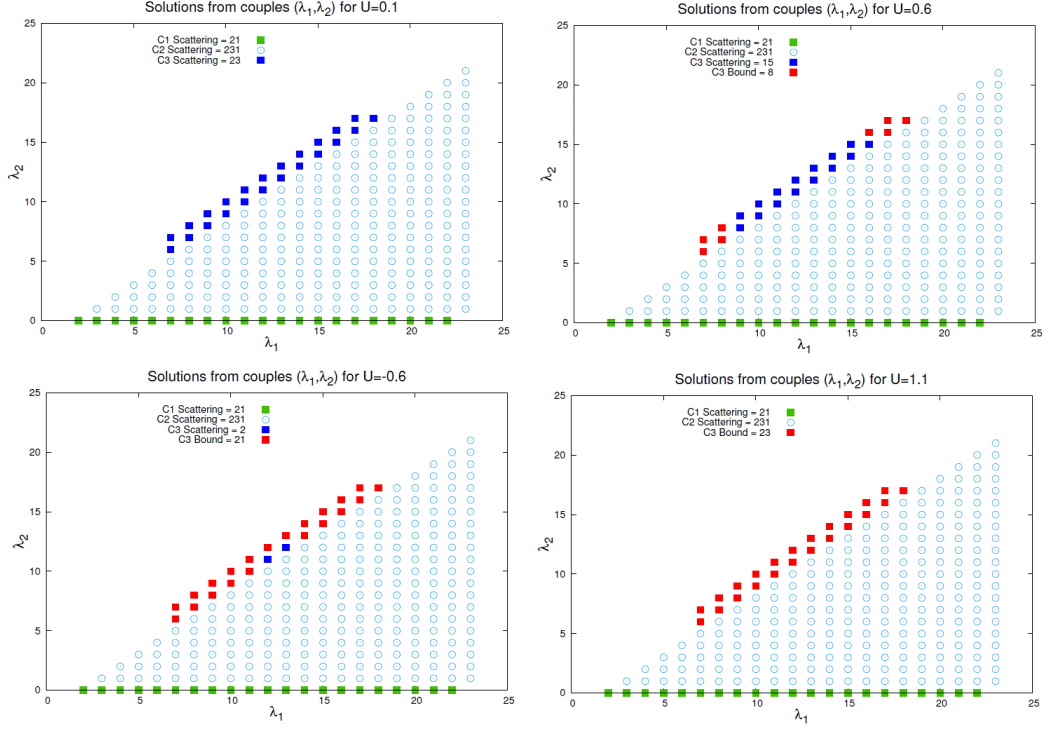
Figure 3.3: Couples of (λ_1, λ_2) for which there is a solution to the Bethe equation for $L = 24$ and $U < 0$.

Figure 3.4: Couples of (λ_1, λ_2) for which there is a solution to the Bethe equation for $L = 24$ and $U > 0$.

The number of solutions from C1 and C3 couples is strongly dependent on the values of U. For example, considering the C3 class solutions, we found that their presence is dependent from U and from and $(\lambda_1 + \lambda_2)$: if $U > 0$ there will be solutions only from couples (λ_1, λ_2) for which held $(\lambda_1 + \lambda_2) < \frac{L}{2}$ or $(\lambda_1 + \lambda_2) > \frac{3L}{2}$; if $U < 0$ there will be solutions only from couples (λ_1, λ_2) for which held $\frac{L}{2} < (\lambda_1 + \lambda_2) < \frac{3L}{2}$. Note that the inequalities are strict. The dependence of the number of solution from L and U is explained in the following table:

	L even		L odd	
	$U < 0$	$U > 0$	$U < 0$	$U > 0$
C1 sols	L	$L - 3$	L	$L - 3$
C3 sols	$L - 4$	$L - 1$	$L - 3$	L
C2 sols	$\frac{L}{2}(L - 5)$	$\frac{L}{2}(L - 5)$	$\frac{L}{2}(L - 5)$	$\frac{L}{2}(L - 5)$
Total	$\frac{L}{2}(L - 1) - 1$	$\frac{L}{2}(L - 1) - 1$	$\frac{L}{2}(L - 1)$	$\frac{L}{2}(L - 1)$

Table 3.1: Number of solutions obtained for class C1, C2 and C3.

This table put a spotlight on the number of solutions, note that the number of total solutions found via numerical evaluation is different between the L odd and the L even case, if L is even there is one less solution than expected.
This is due to a lack of the numerical evaluation, the "missed" C3 solution can be found in the following way.

Consider eq. (3.1) with $\lambda_1 - \lambda_2 = 0$, $\lambda_1 + \lambda_2 = \frac{L}{2}$ so $\lambda_1 = \frac{L}{4}$:

$$-\frac{\frac{U}{t}e^{-\frac{\beta}{L}}e^{i\frac{\alpha}{L}}}{\frac{U}{t}e^{\frac{\beta}{L}}e^{-i\frac{\alpha}{L}}} = e^{-\beta}e^{i(\frac{\pi L}{2} + \alpha)} \tag{3.3}$$

which become:

$$\frac{U}{t}(e^{-\frac{\beta}{L}}e^{i\frac{\alpha}{L}} + e^{-\beta(1-\frac{1}{L})}e^{i\frac{\pi L}{2}}e^{i\alpha(1-\frac{1}{L})}) = 0 \tag{3.4}$$

taking real and immaginary part separately and considering that L is even:

$$e^{-\frac{\beta}{L}}\cos(\frac{\alpha}{L}) + e^{-\beta(1-\frac{1}{L})}\cos(\frac{\pi L}{2})\cos(\alpha(1 - \frac{1}{L})) = 0 \tag{3.5}$$

$$e^{-\frac{\beta}{L}}\sin(\frac{\alpha}{L}) = 0 \tag{3.6}$$

so:

$$\alpha = 0 \tag{3.7}$$

$$\beta = \frac{L}{L - 2}\ln\left(-\cos(\frac{\pi L}{2})\right) \tag{3.8}$$

The eq.(3.8) tells us that for $L = 4m$ with $m \in \mathbb{N}$ the logarithm would have

a negative argument so the solutions doesn't exist, for $L = 2m$ with $m \in \mathbb{N}$ and m odd the solution exist but with $\beta = 0$.

Actually, there is another way to find a solution for eq.(3.3), one could set $\beta = 0$ and search for a scattering solution.
So:

$$\frac{U}{t}(e^{i\frac{\alpha}{L}} + e^{i\frac{\pi L}{2}}e^{i\alpha(1-\frac{1}{L})}) = 0 \qquad (3.9)$$

which gives:

$$\alpha = -\frac{\pi L^2}{2(L-2)} + \pi\frac{L}{(L-2)} \qquad (3.10)$$

but this solution is not allowed because of eq.(3.2).

3.1   Bound state solutions

A bound state is represented by a solution with a purely immaginary relative momentum $p = i\beta$. These are also known as string solutions.
Within a spin picture, the bound state of two flipped spins (or magnons) can be reviewed as a spin wave excitation.
In absence of external applied field (or equivalently for a null chemical potential), for $U \neq 0$ there could be some bound state solutions. As $|U|$ increases, the number of bound state solutions increases too.
The maximum number of bound state solutions is reached for a certain value of U (U^{MAX}) which depend on L. U^{MAX} tends to the unity for $L \to \infty$.

Note that the value of U^{MAX} is different if $U < 0$ or $U > 0$. Denoting with $U_{<0}^{MAX}$ the value of U for which the maximum number of bound state solutions is obtained if $U < 0$ and with $U_{>0}^{MAX}$ the value of U for which the maximum number of bound state solutions is obtained if $U > 0$, so $\left|U_{>0}^{MAX}\right| > \left|U_{<0}^{MAX}\right|$.
In other words, the maximum number of bound state solutions is reached with a "weaker" value of interaction in the case of attractive interaction than the repulsive one.

The number of solutions vs U is reported in fig. (3.5).
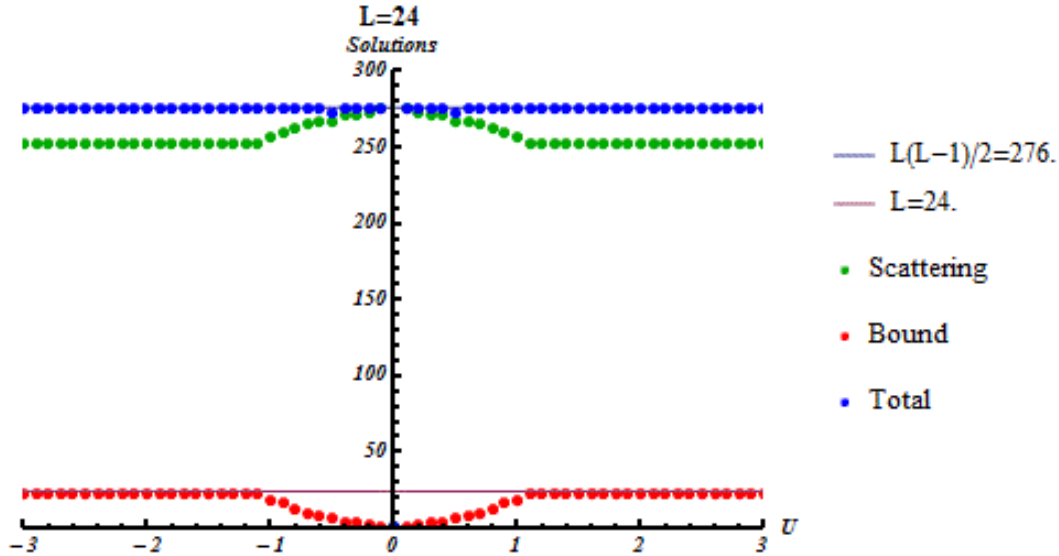
Figure 3.5: Number of solutions obtained vs U. Note that the blue dots (total number of solutions) is always under the blue line (expected number of total solutions).

The energy spectrum is obtained via eq. (2.13).
The energy spectrum, calculated for values of the momentum of the center of mass from 0 to 2π, exhibit the characteristic scattering band. The energies related to the bound states form a new band of energy which is located under the scattering band for $U < 0$ and above the scattering band for $U > 0$.
Moreover, if the parameter U is sufficiently negative, the ground state of the system is represented by a bound state with center of mass momentum $P = 0$ and all the bound state solutions for a given value of P, possesses an energy lower than the scattering solutions for the same P.
In figs (3.6,3.7,3.8,3.9) is reported the energy spectrum vs P (total momentum) and there is the prediction for the energy of the bound states in the thermodynamic limit calculated by eq. (2.36).
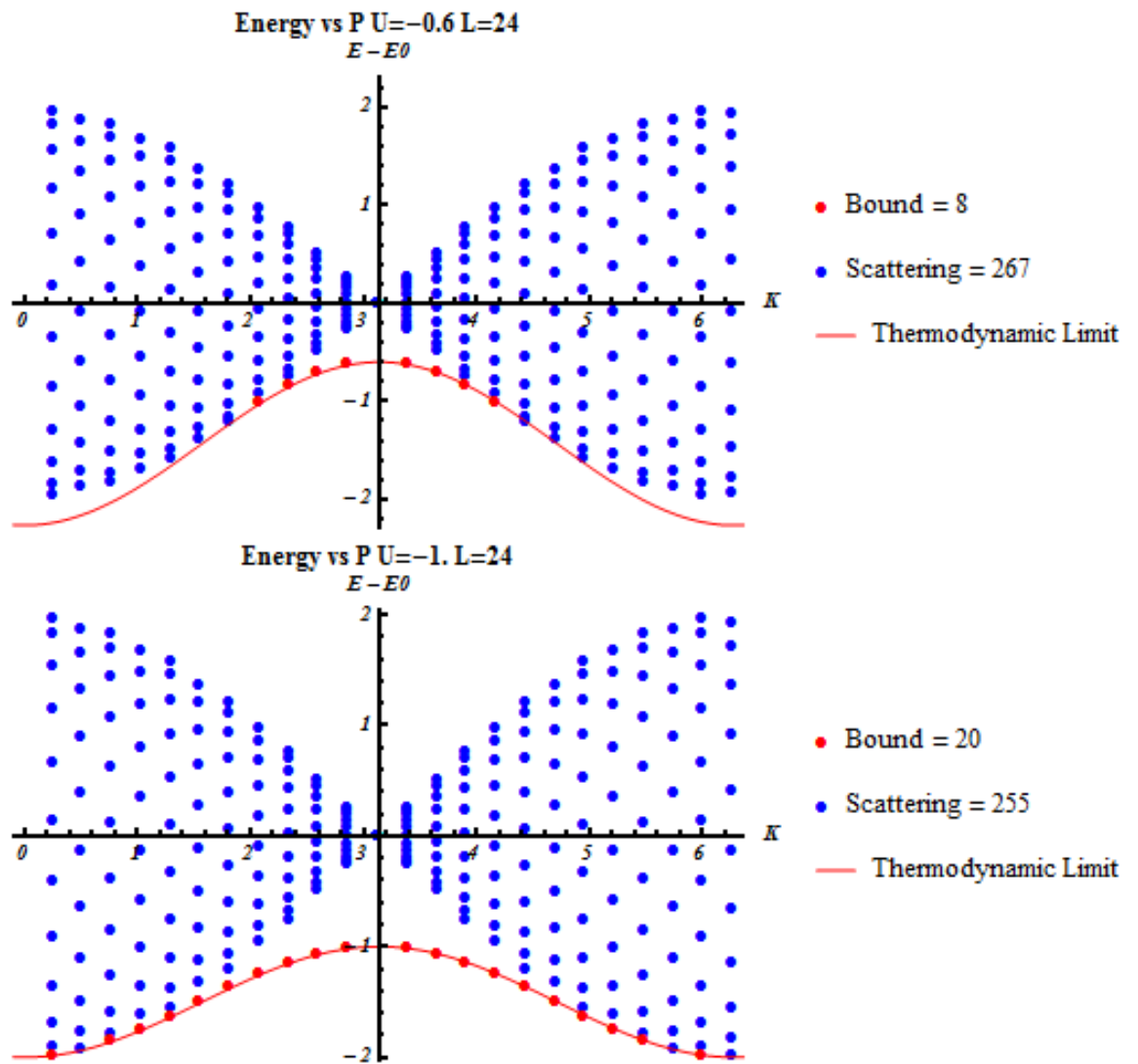
Figure 3.6: Energy spectrum for negative values of U for $L = 24$ with the prediction in the thermodynamic limit for the energy of bound states.

Figure 3.7: Energy spectrum for negative values of U for $L = 24$ with the prediction in the thermodynamic limit for the energy of bound states.

Figure 3.8: Energy spectrum for positive values of U for $L = 24$ with the prediction in the thermodynamic limit for the energy of bound states.

Figure 3.9: Energy spectrum for positive values of U for $L = 24$ with the prediction in the thermodynamic limit for the energy of bound states.
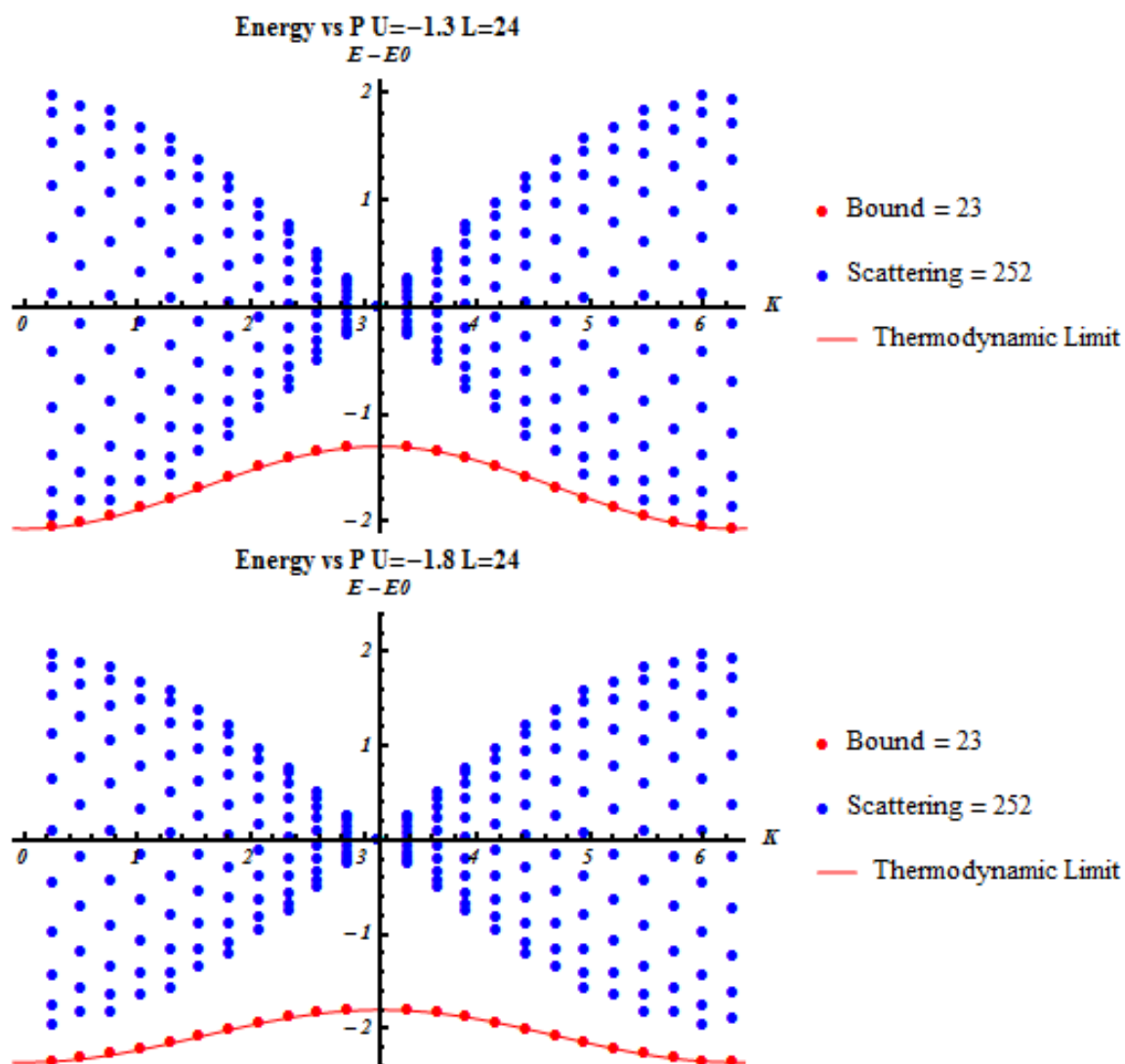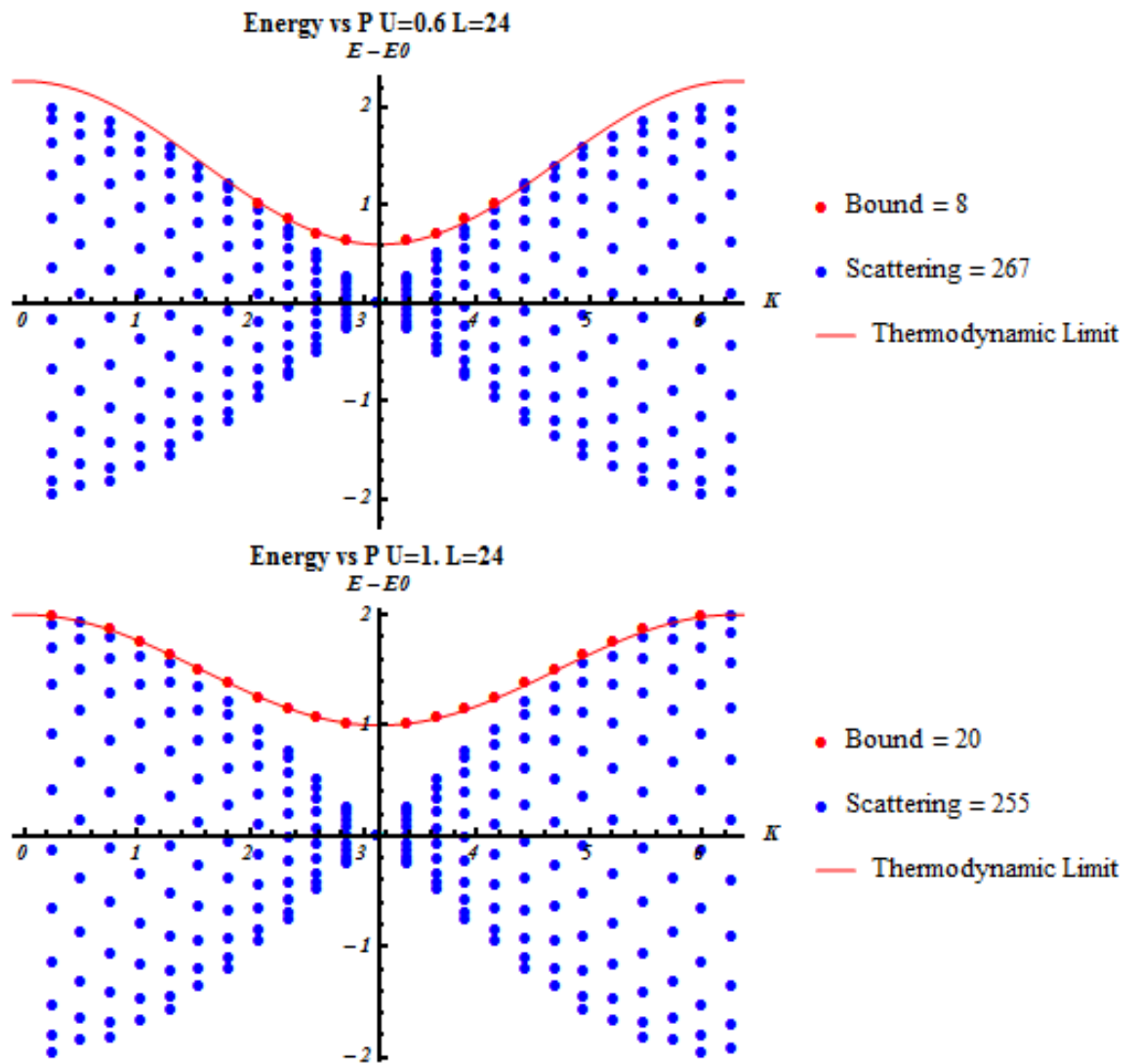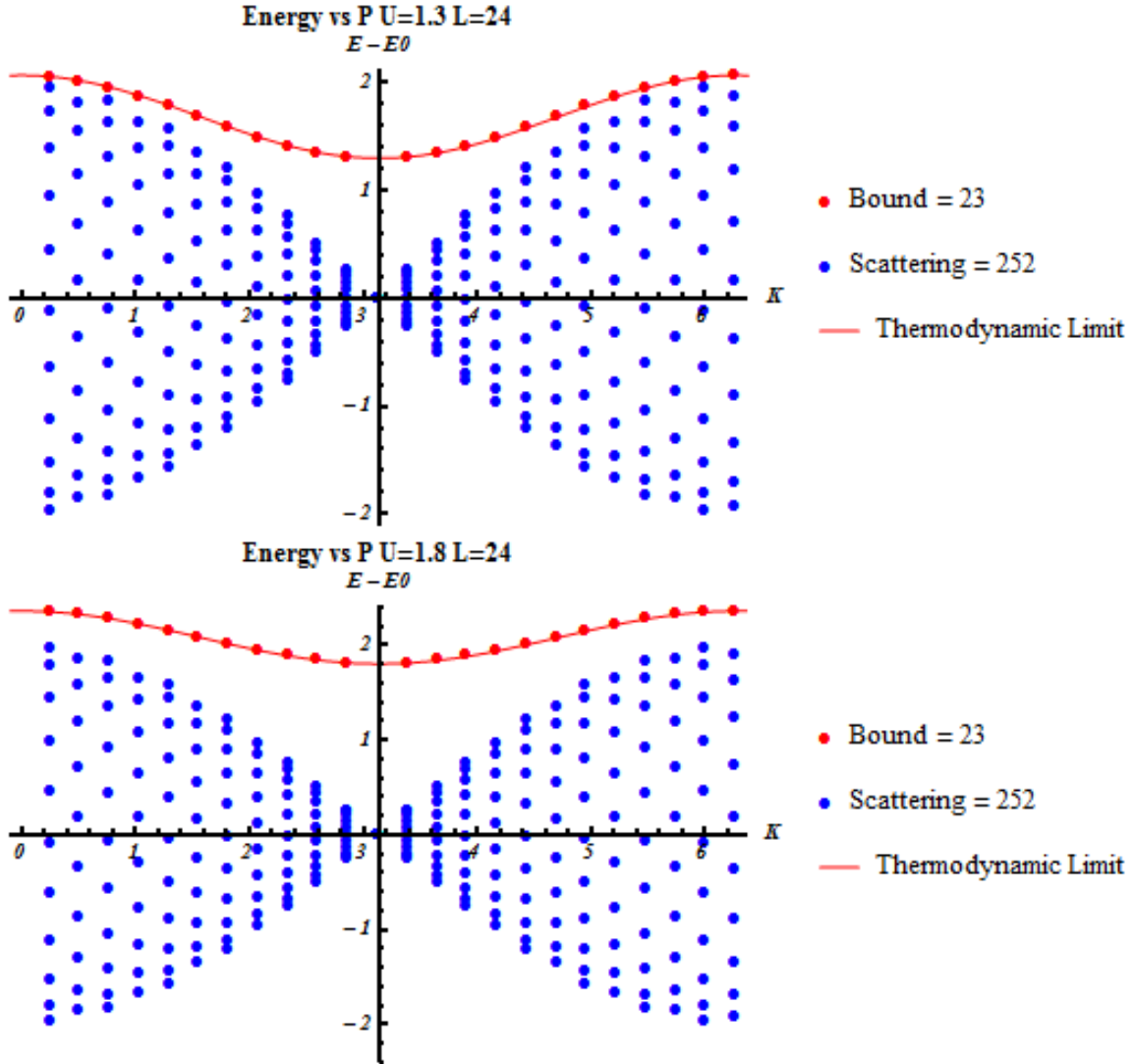
One can also evaluate the difference between the value of the energy of the bound states predicted from the thermodynamic limit in eq. (2.36) and the value obtained substituting in eq (2.13) the momenta of a bound state solution.

Thus we runned different simulation at fixed U ($U = 1.8$) but at different L evaluating the difference $|E_{P=0}^{Bound} - E^{TDLim}|$ for the bound state given from the solution with null center of mass momentum ($P = 0$), plotting this quantity in funciont of L one obtain which shows that for an intermediate value of L as for example $L = 22$ the difference $E_{P=0}^{Bound}$ and E^{TDLim} is beyond the 4th
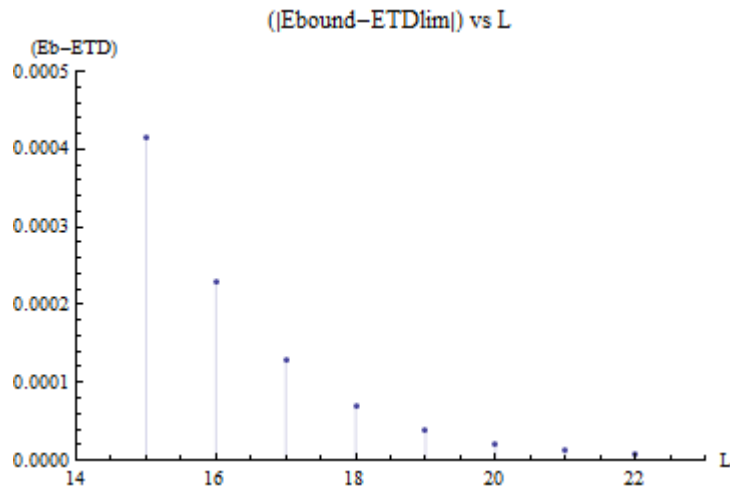
Figure 3.10: Difference between $E_{P=0}^{Bound}$ and E^{TDLim} vs L. It is evident that for big L the Bethe ansatz prediction for the enrgy of the bound states approaches to the thermodynamic prediction

decimal digit.

Chapter 4

Dynamical evolution and numerical simulation

The study of the time evolution of a model brings to understand the dynamics of the model and one can in turn obtain a prediction for some features of the model.

The recent possibility of trapping ultra-cold atoms in optical lattices gives the possibility to simulate fermionic or bosonic interacting systems by changing the interaction parameter.

This stimulated a great theoretical interest toward the study of the dynamics of such systems to compare theoretical or numerical predictions with experimental data.

A recent work from Bonnes et al. studied the dynamics of a spin $\frac{1}{2}$ XXZ chain after a quantum quench[4]. They prepare the system in an initial state which is an eigenstate of the hamiltonian:

$$H_{XXZ}(\Delta_i) = -J \sum_{j=1}^{L} (S_j^x S_{j+1}^x + S_j^y S_{j+1}^y + \Delta_i S_j^z S_{j+1}^z) \qquad (4.1)$$

with Δ_i being the value of the anisotropy before the quench.

Then they let the system evolve with a new value of the anisotropy (Δ_f), all of their quenching protocols imply $\Delta_f < \Delta_i$.

They study the longitudinal spin correlation $S_j^z(t)$ given by:

$$S_j^z(t) = \langle S_{L/2}^z(t) S_j^z(t) \rangle - \langle S_{L/2}^z(t) \rangle \langle S_j^z(t) \rangle \qquad (4.2)$$

where $L/2$ is the position of the middle site of the chain.

What turns out from the study is that $S_j^z(t)$ exhibit the tipycal "light-cone"

effect with a spreading speed being dependent from both the value of Δ_i and Δ_f.

This result means that it is not only the quenched evolving hamiltonian that determines the dynamics of the system but the initial state matter too.

In the same direction there is a work from Degli Esposti Boschi et al[5]. for the study of expansion dynamics of bosons on a 1D lattice.
The hamiltonian is the following

$$H_B = -J \sum_{j=1}^{L} (b_j^+ b_{j+1} + b_{j+1}^+ b_j) + \frac{U}{2} \sum_{j=1}^{L} n_j(n_j - 1) \qquad (4.3)$$

with b_j being the bosonic annihilation operator and $n_j = b_j^+ b_j$.
In this study, considering the case of two particles, the authors are able to obtain the exact eigenvalues with a Bethe ansatz approach with scattering and bound states solutions.
This allows to identify the effects of the presence of the bound states on the dynamics of the system.
The study is focused on the evolution of the density $(\rho_j(t))$, the single occupation $(s_j(t))$ and the double occupation $(d_j(t))$ on the lattice given by:

$$\rho_j(t) = \langle \Psi(t)| \frac{n_j}{2} |\Psi(t)\rangle \qquad (4.4)$$

$$s_j(t) = \langle \Psi(t)| n_j(2 - n_j) |\Psi(t)\rangle \qquad (4.5)$$

$$d_j(t) = \langle \Psi(t)| \frac{n_j(n_j - 1)}{2} |\Psi(t)\rangle \qquad (4.6)$$

What turns out is that the spreading velocity is strongly influenced by the presence of bound states, as one could intuitively expect the larger the projection of the initial state on bound state the smaller the spreading velocity.
Another curious feature is the behaviour of the bosons with the different values of U, as shown in the paper for $U = 0$ the density profile follows a free expansion, it changes as the U is changed and tends to become again a free expansion profile for large U.
This is explained by authors with the fact that bosons with a large interaction parameter tend to become hard-core bosons and in this case they are equivalent to free (fermionic) particles.

In our study we would try to extend these results to the fermionic case which is represented from the spinless fermion 1D chain, finding the role of

the bound states during the time evolution of the system.

Obviously, by mean of the Wigner-Jordan transformation, the results can be translated directly in the language of spin on a 1D chain.

4.1 DMRG

The description of the physical properties of low-dimensional strongly correlated quantum systems is one of the major tasks in theoretical condensed matter physics.

Due to the large size of the Hilbert space it is in many cases impossible to find an exact solution of the quantum systems. Take as example the problem of two spinless fermions on a 1D chain of lenght L.

For this very simple model, we have only two possible states for every site: absence of particles ($|0\rangle$) and presence of one particle ($|1\rangle$), so the total dimension of the Hilbert space will be 2^L. Even for a short chain with $L = 10$ the system will be described by 1024 states and the problem cannot be easily solved.

So one can try to use a numerical method to diagonalize the hamiltonian and take the exact eigenstate and eigenvalues, actually this could be a very difficult task considering the enormous dimension of the Hilbert space.

In 1992 S. White developed[27][28] the density-matrix renormalization-group method (DMRG) which allowed decisive progress in the description of the low-energy equilibrium properties of 1D strongly correlated quantum systems.

The DMRG method, differently from other renormalization techniques such as the Real-Space Renormalization Group (RSRG), performs an iterative decimation of the Hilbert space based on the evaluation of the density matrix.

In fact, the DMRG at every step of iteration retain only the states which have the highest-weight eigenvalues and so its consider a reduced Hilbert space. We will see in following paragraphs this and the others approximation methods in details.

This approximation allows to solve numerically the system with a good degree of fidelity and using a reasonable amount of time and computational resources.

The DMRG method has yielded an enormous wealth of information on the static and dynamic equilibrium properties of one-dimensional systems[23] and

is one of the most powerful computational methods.

4.2   DMRG method

The density-matrix renormalization group (DMRG) is a numerical method
to study low-dimensional strongly correlated systems.
The DMRG algorithm belongs to the family of the "renormalization meth-
ods". Starting from some microscopic Hamiltonian it iteratively integrates
out degrees of freedom, such that an effective description of the system is
obtained.
The difficulty is to obtain an effective description without loose any physical
feature.
The "renormalization method" works as follows: start from a chain (also
called "block") of length l sufficiently small to be represented numerically on
a computer.
Then the chain is enlarged until the desidered lenght L is reached. The en-
larging procedure is performed step by step adding one (in some rare cases
more than one) site per time, the dimension of the Hilbert space is reduced
taking only the portion of the Hilbert space in which there are the most
"relevant" states.
The problem is to define which are the "relevant" states.
For example, in the Real-Space Renormalization Group method (RSRG), the
decimation procedure of the Hilbert space is to take the lowest-lying eigen-
states of the compound block AA (Fig. 4.1). This bring to a description of
the ground state of the entire chain essentially with the energetically low-
lying states of smaller blocks. This RSRG procedure gives very poor results,
its failure can be explained in that way (Fig. 4.1): assuming a rather large
block size, where discretization can be neglected, the lowest-lying states of
A will have their nodes at the lattice ends, such that all product states of
AA will have nodes at the compound block center. The true ground state
of AA will have its maximum amplitude right in the block center, such that
the properly approximation cannot be obtained with a restricted number of
block states.

So, considering isolated blocks imposes wrong boundary conditions. White
and Noack in 1992 realized that one could obtain excellent results by consid-
ering that the presence of the "environment".
In the DMRG method there are two growing blocks, one representing the
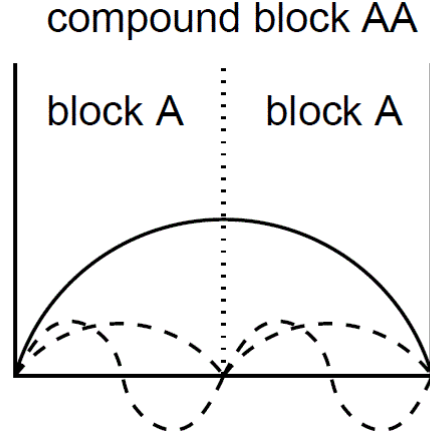
compound block AA

Figure 4.1: Two blocks A are connected to form the compound block AA. The dashed lines are the lowest energy eigenstates of the separate blocks A, the solid line represents the lowest energy eigenstate of the compound block AA. Fig. from [23]

system (S) and one representing the environment (E).

These block start from an initial lenght l and are enlarged both of one site, so at every enlargment step the total system is composed by the block S, two sites and the block E. We thus arrive to what is called a "superblock" of length $2l + 2$ (Fig. 4.2)

The last step of the enlargment procedure is when a superblock of lenght L is obtained.

Assuming that for a block of length l we have an M^S-dimensional Hilbert space with states $\{|m_l^S\rangle\}$. The Hamiltonian $\widehat{H}_l$ is given by matrix elements $\langle m_l^S|\widehat{H}_l|m_l^S\rangle$ Similarly we know the matrix representations of local operators such as $\langle m_l^S|\widehat{o}_i|m_l^S\rangle$.

For linear growth, we can now write $\widehat{H}_{l+1}$ in the product basis

$$\{|m_l^S\sigma\rangle\} = \{|m_l^S\rangle|\sigma^S\rangle\} \tag{4.7}$$

where $|\sigma^S\rangle$ are the N_{site} local states of a new site added.

At this point, one can obtain the ground state of the superblock by a numerical diagonalization:

$$|\psi\rangle \quad = \quad \sum_{m^S=1}^{M^S}\sum_{\sigma^S=1}^{N_{site}}\sum_{\sigma^E=1}^{N_{site}}\sum_{m^E=1}^{M^S} \psi_{m^S\sigma^S\sigma^E m^E}|m^S\rangle|\sigma^S\rangle|m^E\rangle|\sigma^E\rangle \tag{4.8}$$

$$\implies \quad |\Psi\rangle \equiv \sum_{i}^{N^S}\sum_{j}^{N^E}\psi_{ij}|i\rangle|j\rangle \qquad \langle\psi|\psi\rangle = 1$$

where $\psi_{m^S \sigma^S \sigma^E m^E} = \langle m^S \sigma^S ; \sigma^E m^E | \psi \rangle$.

$\left\{ | m^S \sigma^S \rangle \right\} = \{ |i\rangle \}$ and $\left\{ | m^E \sigma^E \rangle \right\} = \{ |j\rangle \}$ are the orthonormal product bases of system and environment (subscripts have been dropped) with dimensions $N^S = M^S N_{site}$ and $N^E = M^E N_{site}$ respectively. In general $N^S \neq N^E$.
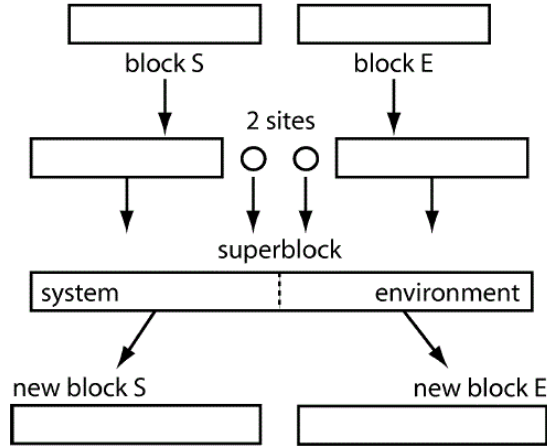
Figure 4.2: DMRG construction of a superblock from two blocks and two single sites. Fig. from [23]

Some truncation procedure from N^S to $M^S < N^S$ states must now be implemented.

The first way to obtain a good truncation is to perform an optimization of expectation values.

If the superblock is in a pure state $|\psi\rangle$ given by eq. (4.8), the physical state of the system can be described through a reduced density-matrix $\widehat{\rho}$

$$\widehat{\rho} = Tr_E |\psi\rangle\langle\psi| \tag{4.9}$$

where the states of the environment have been traced out.

So

$$\langle i | \widehat{\rho} | k \rangle = \sum_j \psi_{ij} \psi^*_{kj} \tag{4.10}$$

$\widehat{\rho}$ has N^S eigenvalues w_α and orthonormal eigenstates so that

$$\widehat{\rho} | w_\alpha \rangle = w_\alpha | w_\alpha \rangle \tag{4.11}$$

with $\sum_\alpha w_\alpha = 1$ and $w_\alpha \geq 0$.
We assume the states are ordered such that $w_1 \geq w_2 \geq w_3 \geq \ldots$
Now we can approximate the ground state of the system retaining only those states of M^S with largest weight w_α.
It can be shown[23] that the error ϵ_ρ for local quantities, such as energy, magnetization or density, are of the order of the truncated weight

$$\epsilon_\rho = 1 - \sum_{\alpha=1}^{M^S} w_\alpha \qquad (4.12)$$

Hence, a fast decay of density matrix eigenvalues w_α will bring to better performance of this truncation procedure.

Another method implemented in the DMRG for truncation of the Hilbert space is the optimization[27][28][23] of the wave function.
This, starting from the only requirement that quantum mechanical objects are completely described by their wave function, require that the approximate wave function $|\widetilde{\psi}\rangle$ where the system space has been truncated to be spanned by only M^S orthonormal states $|\alpha\rangle = \sum_i u_{i\alpha}|i\rangle$

$$|\widetilde{\psi}\rangle = \sum_{\alpha=1}^{M^S} \sum_{j=1}^{N^E} a_{j\alpha}|\alpha\rangle|j\rangle \qquad (4.13)$$

minimizes the distance in the quadratic norm

$$\left|\left||\psi\rangle - |\widetilde{\psi}\rangle\right|\right| \qquad (4.14)$$

White[27] found that choosing $|\alpha\rangle$ to be the M^S eigenvectors $|w_\alpha\rangle$ with the largest eigenvalues w_α of the density matrix, the minimal distance squared is:

$$\left|\left||\psi\rangle - |\widetilde{\psi}\rangle\right|\right|^2 = 1 - \sum_{\alpha=1}^{M^S} w_\alpha \qquad (4.15)$$

which is equal to ϵ_ρ.

The last method used for the truncation of the Hilbert space is the optimization of entanglement.

It has been found[10][18][22] that the truncation procedure described above ensures the maximum entanglement system-environment.

Using the von Neumann entropy for the measure of the entanglment one can obtain

$$S_{vN} = -Tr\widehat{\rho}\ln_2\widehat{\rho} = -\sum_{\alpha=1}^{N_{Sch}} w_\alpha \ln_2 w_\alpha \qquad (4.16)$$

where N_{Sch} is the number of states used to describe the system $|\psi\rangle$ after a Schmidt decomposition for which the reduced density matrices for system and environment are given by

$$\widehat{\rho}_S = \sum_{\alpha=1}^{N_{Sch}} w_\alpha |w_\alpha^S\rangle\langle w_\alpha^S| \qquad (4.17)$$

$$\widehat{\rho}_E = \sum_{\alpha=1}^{N_{Sch}} w_\alpha |w_\alpha^E\rangle\langle w_\alpha^E| \qquad (4.18)$$

Note that generally $N_{Sch} \leq \min(N^S, N^E)$

Using DMRG one can obtain a good estimation for the energy of the system and for the expectation values for n-point correlations.

As a method working in a subspace of the full Hilbert space, the DMRG results to be variational in energy. The value obtained for energies $E(M)$ improves monotonically with M, the number of basis states in the reduced Hilbert space.

Rerunning the calculation of a system of size L for various M, one observes for sufficiently large values of M that to a good approximation the error in energy per site scales linearly with the truncated weight[23],

$$\frac{E(M) - E_{exact}}{L} \propto \epsilon_\rho \qquad (4.19)$$

with a non-universal proportionality factor typically of order 1 to 10, sometimes more[29][19].

As ϵ_ρ is often of order 10^{-10} or less, DMRG energies can thus be extrapolated using Eq. (4.19) quite reliably to the exact $M = \infty$ result, often almost at machine precision. The precision desired imposes the size of M, which for spin problems is typically in the lower hundreds, for electronic problems in the upper hundreds, for two-dimensional and momentum-space problems in

the lower thousands.

For what concern the evaluation of properties, the DMRG is able to calculate the expectation value of a n-point correlation operator[23]

$$\widehat{O}_{i_1\ldots i_n}^{(n)} = \widehat{O}_{i_1}^{(1)}\ldots\widehat{O}_{i_n}^{(1)} \tag{4.20}$$

for most pratical purpose the interesting cases are $n = 1$ and $n = 2$.
With $n = 1$ one can measure properties like density or local magnetization. The growth strategy of DMRG bring to a three-step procedure of initializing, updating and evaluating correlators.
During the inizialization $\widehat{O}_i$ acts on site i, when this site is added to a block of length $l - 1$ the quantity $\langle\sigma|\widehat{O}_i|\widetilde{\sigma}\rangle$ is evaluated.
With $\{|m_l\rangle\}$ being the reduced basis of the new block enlarged with site i and $\{|m_{l-1}\rangle\}$ the basis of the old block, one has

$$\langle m_l|\widehat{O}_i|\widetilde{m}_l\rangle = \sum_{m_{l-1}\sigma\widetilde{\sigma}} \langle m_l|m_{l-1}\sigma\rangle\langle\sigma|\widehat{O}_i|\widetilde{\sigma}\rangle\langle\widetilde{m}_{l-1}\widetilde{\sigma}|\widetilde{m}_l\rangle \tag{4.21}$$

where $\langle m_l|m_{l-1}\sigma\rangle$ is already known from the density-matrix eigenstates.
Hence start the update phase, a basis transformation for the block containing the site where $\widehat{O}_i$ is carried. As $\widehat{O}_i$ does not act on the new site, the operator transforms as

$$\langle m_{l+1}|\widehat{O}_i|\widetilde{m}_{l+1}\rangle = \sum_{m_l\widetilde{m}_l\sigma} \langle m_{l+1}|m_l\sigma\rangle\langle m_l|\widehat{O}_i|\widetilde{m}_l\rangle\langle\widetilde{m}_l\widetilde{\sigma}|\widetilde{m}_{l+1}\rangle \tag{4.22}$$

After the last DMRG step starts the evaluation, $\langle m^S\sigma^S\sigma^E m^E|\psi\rangle$ is known and $\left\langle\widehat{O}_i\right\rangle$ reads, assuming $\widehat{O}_i$ to act on some site in the system block,

$$\langle\psi|\widehat{O}_i|\psi\rangle = \sum_{m^S\widetilde{m}^S\sigma^S\sigma^E m^E} \langle\psi|m^S\sigma^S\sigma^E m^E\rangle\langle m^S|\widehat{O}_i|\widetilde{m}^S\rangle\langle\widetilde{m}^S\sigma^S\sigma^E m^E|\psi\rangle \tag{4.23}$$

If we are interested into measuring 2-point correlation which could mean e.g. a measure of density-density correlations or spin-spin correlation, so we have to deal with the case $n = 2$.
Now two subcases have to be distinguished, whether the locations i and j of the contributing 1-point operators act on different blocks or on the same

block at the last step.

If they act on different blocks, one follows through the procedure for 1-point operators, yielding $\langle m^S | \widehat{O}_i | \widetilde{m}^S \rangle$ and $\langle m^E | \widehat{O}_j | \widetilde{m}^E \rangle$. The evaluation is done by the following modification of eq. (4.23)

$$\langle \psi | \widehat{O}_i \widehat{O}_j | \psi \rangle = \sum_{m^S \widetilde{m}^S \sigma^S \sigma^E m^E \widetilde{m}^E} \langle \psi | m^S \sigma^S \sigma^E m^E \rangle \langle m^S | \widehat{O}_i | \widetilde{m}^S \rangle \langle m^E | \widehat{O}_i | \widetilde{m}^E \rangle \langle \widetilde{m}^S \sigma^S \sigma^E \widetilde{m}^E | \psi \rangle$$

$$(4.24)$$

Instead, if they act on the same block, the difference is in the inizialization. Such operators have to be built as a compound object at the step in which they belong to a product Hilbert space, namely when one of the operators acts on a block of length $l - 1$, the other on a single site, that is being attached to the block. Then we know $\langle m_{l-1} | \widehat{O}_i | \widetilde{m}_{l-1} \rangle$ and $\langle \sigma | \widehat{O}_j | \widetilde{\sigma} \rangle$ and within the reduced bases of the block of length l the eq.(4.21) became

$$\langle m_l | \widehat{O}_i \widehat{O}_j | \widetilde{m}_l \rangle = \sum_{m_{l-1} \widetilde{m}_{l-1} \sigma \widetilde{\sigma}} \langle m_l | m_{l-1} \sigma \rangle \langle m_{l-1} | \widehat{O}_i | \widetilde{m}_{l-1} \rangle$$

$$\langle \sigma | \widehat{O}_j | \widetilde{\sigma} \rangle \langle \widetilde{m}_{l-1} \widetilde{\sigma} | \widetilde{m}_l \rangle$$

$$(4.25)$$

The updating and final evaluation stages for "compound" operators proceed as for a one-point operator.

4.3   DMRG Algorithm

Generally speaking the algorithm for the DMRG has been developed for the simulation of an infinite system.

Here we report the general idea of this algorithm, which is fully explained in [17][23]:

1. Inizialization of the system (S) with a starting lattice of lenght l. The initial states form a basis given by $\{|m_l^S\rangle\}$, at this level the Hamiltonian and the operator acting on the system are assumed to be known. The same is done for the environment (E).

2. Form the new system S' adding a lattice point to S. The Hilbert space dimension of S' is now $N^S = M^S N_{site}$, the new basis is $\{|m_l^S\rangle |\sigma\rangle\}$. The new environment E' is build in the same way from E.

3. Build the superblock of length $2l + 2$ from S' and E'. The Hilbert space is of size $N^S N^E$, and the matrix elements of the Hamiltonian

H_{2l+2} could in principle be constructed explicitly, but this is avoided for efficiency reasons.

4. Find by large sparse-matrix diagonalization of H_{2l+2} the ground state $|\psi\rangle$. This is the most timeconsuming part of the algorithm.

5. Form the reduced density matrix and determine its eigenbasis and eigenvalues. form the reduced basis for S' taking the M^S eigenstates with the largest weights. Proceed in the same way for the environment.

6. Find the new Hamiltonian H_{l+1} for the system and for the environment. Repeat from step 2 until the desired lenght is reached. Update operator representation.

7. Calculate desired ground state properties (energies and correlators) from $|\psi\rangle$. This step can also be carried out at each intermediate length.

However, for many problems infinite-system DMRG does not yield satisfactory answers. DMRG is usually used with fixed particle numbers and finite system size.

The finite system algorithm is based on the idea to stop the infinite-system algorithm at a predefined superblock length L.

So, once the lenght L is reached (Fig. 4.3), the growth is stopped but infinite-system algorithm steps are applied too. Instead of simultaneous growth of both blocks, only one block is allowed to grow at the expenses of the other block. The calculations for the reduced basis transformations are carried out only for the growing block.

For example let us consider this stage: the system block grow from l to $l+1$ at the expense of the environment block which shrink to $k-1$;

to describe it, environment blocks of all sizes and operators acting on this block, expressed in its basis, must have been stored previously.

Once the environment block reaches the minimum size and its description becomes exact, the growth direction is reversed, and the enviroment block grows at the expense of the system. If the system is symmetric under reflection, blocks can be mirrored at equal size, otherwise the shrinking block is reduced until a minumum size is reached and then regrown. A complete shrinkage and growth sequence for both blocks is called a sweep.
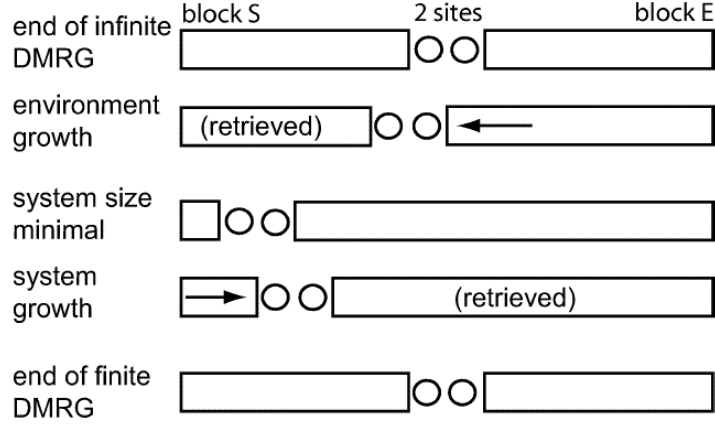
Figure 4.3: Sweep steps of the finite-system DMRG algorithm. Fig. from [23]

4.4   Time evolution of the system and the workframe of the adaptive time dependent DMRG (a-DMRG)

Consider the spinless fermion 1D chain model, in chapter 2 we have obtained the explicit form of the eigenstates in the case of two particles and we know exactly the behaviour of the solutions on U.

The initial state is of the form

$$|\phi(t=0)\rangle = \sum_{j,k=1}^{L} \phi_{j,k} c_j^+ c_k^+ |0\rangle \tag{4.26}$$

With the $\phi_{j,k}$ given from the Bethe ansatz solution.

Now, labelling with s and b the scattering and the bound state solutions respectively we can write a completeness relation:

$$\sum_b |b\rangle\langle b| + \sum_s |s\rangle\langle s| = 1 \tag{4.27}$$

So the initial state can be expressed in term of a linear combination of $|s\rangle$ and $|b\rangle$ states:

$$|\phi(t=0)\rangle = \sum_b C_b^0 |b\rangle + \sum_s C_s^0 |s\rangle \tag{4.28}$$

with $C_b^0 = \langle b|\phi(t=0)\rangle$ and $C_s^0 = \langle s|\phi(t=0)\rangle$ being the coefficient at initial

time.

The time evolution of the system can be studied using the time dependent Schroedinger equation which gives (setting $\hbar = 1$):

$$|\phi(t)\rangle = \sum_b C_b^0 e^{-i\widehat{H}t}|b\rangle + \sum_s C_s^0 e^{-i\widehat{H}t}|s\rangle \qquad (4.29)$$

The evolution will be obtained with time evolving Density Matrix Renormalization Group (DMRG or equivalently DMRGTEV) techniques. Here we evaluate the evolution of the system on the basis of a Runge-Kutta approximation using the infinitesimal time-evolving operator, so:

$$|\phi(t + \Delta t)\rangle = (1 - i\widehat{H}\Delta t)|\phi(t)\rangle \qquad (4.30)$$

where Δt is the time step of the evolution.

In the computational study of the dynamical evolution of a physical system one should account very carefully to what is happening during the simulation. The results are affected by errors which rise by the natural numerical approximation, e.g. a calculator which has a finite number of bits to represent a real (infinite digits) number, and from the approximation which came from the numerical methods we are implementing.
Although one cannot do nothing for first issue, the latter depends only on the algorithm used to estimate the evolved state.
The first peculiarity of the a-DMRG we would like to display is the fact that the Hilbert space considered during the evolution is "adapted" to the evolved state.
So, the dimension of the Hilbert space considered is held constant and it is always smaller than the dimension of the total Hilbert space.
This is based on the reasonable idea that if $\widetilde{H}$ is the total Hilbert space of the system the initial state $|\Psi(t = 0)\rangle$ can be descripted with a reduced subspace $\widetilde{H}_0$. Now, if the system evolves toward a new state $|\Psi(t = \Delta t)\rangle$ to describe the evolved state one could use an enlarged subspace of the kind $\widetilde{H}_{\Delta t} = \widetilde{H}_0 + \delta\widetilde{H}$ retaining all the subspace of the previous state.
This bring to an incontrolled growth of the subspace considered which cause a useless growth of the computational time and consumption of computational resources.
Instead, the a-DMRG perform a stage of optimization of the subspace considered "adapting" the subspace to the evolved state. So at every step in the new subspace there will be only the "vectors" which best describe the

evolved state (Fig. 4.4)
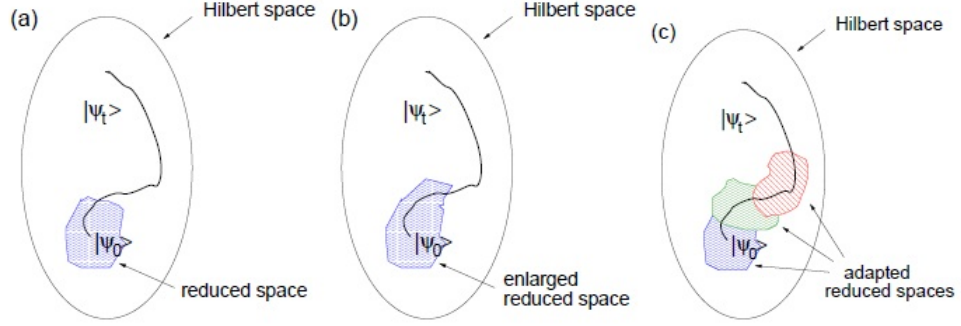
Figure 4.4: a) the subspace of the initial state; b) the enlarged subspace for first steps of evolution; c) the "adapted" subspaces for first steps of evolution. Fig. from [17]

For what concern the evaluation of the evolved state, the DMRG proceed implementing a 4th order Runge-Kutta algorithm to every DMRG step.
Let us consider a typical next-neighbour interacting hamiltonian, it can be splitted into the sum of two hamiltonian of the kind:

$$H = F + G = \sum_i F_{i,i+1} + \sum_j G_{j,j+1} \qquad (4.31)$$

Where i and j are respectively an even integer and an odd integer, thus $F_{i,i+1}$ is the hamiltonian which describes the interaction between a couple of next-neighbour sites with i even (even bond) and $G_{j,j+1}$ is the hamiltonian which describes the interaction between a couple of next-neighbour sites with j odd (odd bond). All the terms of F and G commute each other but terms which share one site.
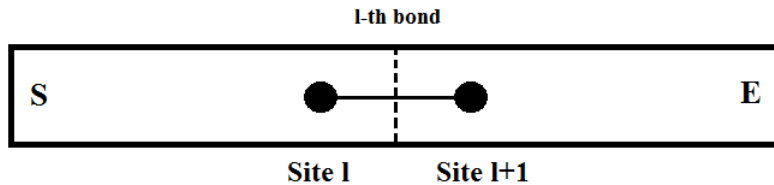The evolution operator can be represented with a first order Trotter expansion in this way:

$$e^{-iH\delta t} = \prod_i e^{-iF_{i,i+1}\delta t} + \prod_j e^{-iG_{j,j+1}\delta t} + O(\delta t^2) \qquad (4.32)$$

So, the time evolution in the a-DMRG is evaluated at each time step trought the local evolution operator (LEO) $e^{-iF_{i,i+1}\delta t}$ and $e^{-iG_{j,j+1}\delta t}$
Using a second order Runge-Kutta approximation the evolved state is expressed by:

$$|\Psi(t+\delta t)\rangle = (1 - iH\delta t)|\Psi(t)\rangle \qquad (4.33)$$

Figure 4.5: Partitioning the lattice for the time evolution. Fig. from [17]

The simulation starts implementing the finite-size DMRG algorithm which "build up" the lattice of the desidered lenght and compute the ground state for the hamiltonian at $t = 0$.

Once the time starts the LEO is applied to the even bond of the state $|\Psi(t)\rangle$, the LEO can be applied only when the system is in the right configuration of two sites-two blocks.

In order to get the right configuration, the lattice is splitted at the bound between points l and $l+1$. This i.e. to have a system block of lenght $l-1$, a point (site) l, a point (site) $l+1$ and an environment block of lenght $L-l-1$ (Fig. 4.5).

This allows to apply the LEO for the bound between l and $l+1$ once the evolved state is obtained a DMRG truncation of the Hilbert space is performed in order to adapt the dimension of the Hilbert space to the evolved state.

Then the next even bond is splitted (e.g. the bond between $l+2$ and $l+3$) until the end of the chain is reached, this is called a sweep.

Once the end of the chain is reached another sweep starts in the opposite direction but this time the evolved bonds are the odd.

When all the bonds are updated the algorithm proceed to evaluate the operators (properties) given in the input.

Chapter 5

New results and outlooks

In our case of study the a-DMRG method has been applied to the two particles SF model hamiltonian. The quenching protocol is quite simple: the starting hamiltonian is defined with $U = 0$ and a large chemical potential on central sites, in the final hamiltonian an interacting potential is turned on and the chemical potential is switched off. The hopping parameter t is set on unity.
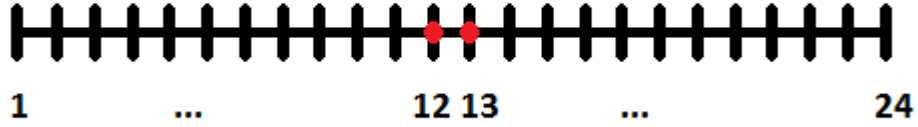
$$H^0(t \; = \; 0) = -\frac{1}{2} \sum_{i=1}^{L} \left(c_i^+ c_{i+1} + c_{i+1}^+ c_i \right) + \mu(n_{\frac{L}{2}} + n_{\frac{L}{2}+1}) \qquad (5.1)$$

$$H(t \; \neq \; 0) = -\frac{1}{2} \sum_{i=1}^{L} \left(c_i^+ c_{i+1} + c_{i+1}^+ c_i \right) + U \sum_{i=1}^{L} n_i n_{i+1} \qquad (5.2)$$

This quenching protocol has been applied with several values of U ranging from $U = -4$ to $U = 4$ with a starting product state given by the ground state of H^0:

$$|\Psi_{PS}\rangle = c_{\frac{L}{2}}^+ c_{\frac{L}{2}+1}^+ |0\rangle \qquad (5.3)$$

which correspond to a wave packet of two fermions on the central sites of the chain. The value of L used is $L = 24$.

Figure 5.1: A 24 sites lattice with two fermions "sitting" on central sites

This configuration is equivalent to the spin configuration of [4] and is the fermionic translation of the first case of [5].

Free particle case $U = 0$
Evaluating the expectation value of the density at every instant of the simulation one can visualize the spreading of the wave packet during the evolution. Let us start evaluating the spreading of a system of free fermion in which in the evolving hamiltonian the interaction parameter is $U = 0$.
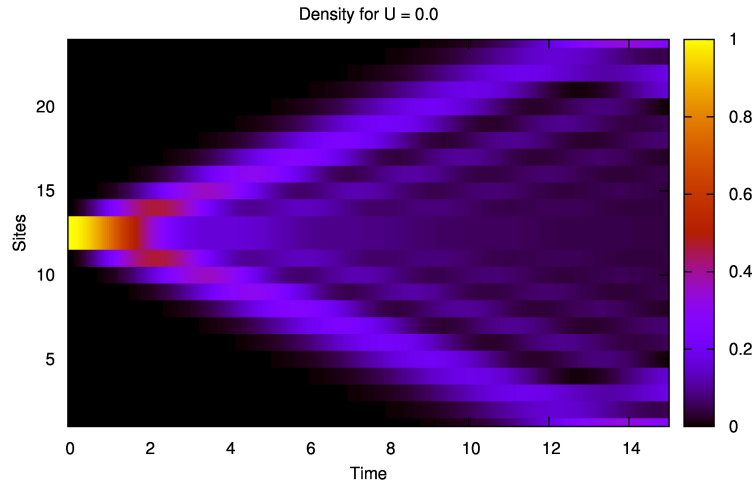
Figure 5.2: Density profile of a system of free fermions with PBC.

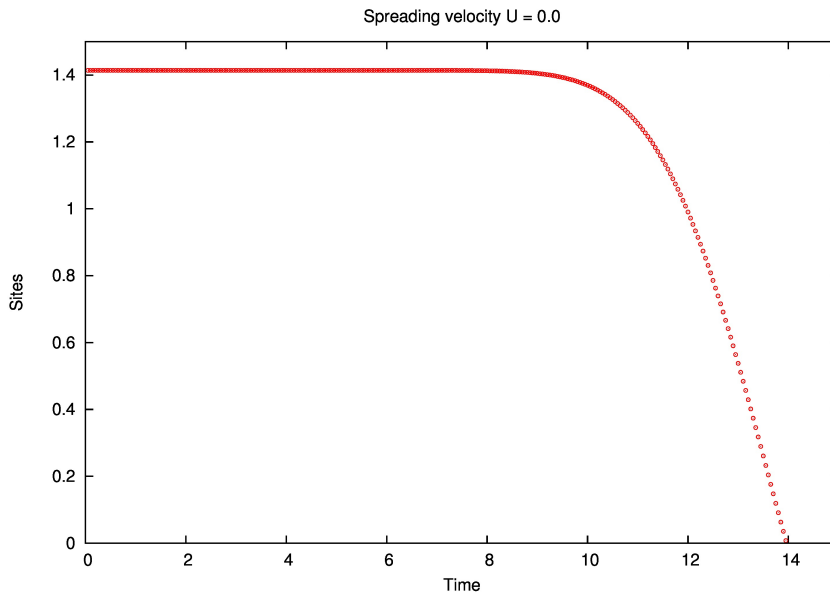The wave packet spreads all along the chain, one could estimate the spreading velocity calculating:

$$v = \frac{d}{dt}\sqrt{R^2(t) - R^2(t = 0)} \tag{5.4}$$

where $R^2(t)$ is the time-dependent variance of the density distribution

$$R^2(t) = \frac{1}{N}\sum_{i=1}^{L} n_i(t)(i - i_0)^2 \tag{5.5}$$

here i_0 is the centre of the wave packet at $t = 0$.
Plotting the spreading velocity in function of the time for $U = 0$, one obtain:

Figure 5.3: Spreading velocity of a system of free fermions with PBC.

in fig. (5.3) it is possible to see that the wave packet spread out with constant speed $v = \sqrt{2}$, this value is obtained also in [5] as spreading speed for the free bosonic particles case. The decreasing tail in fig. (5.3) is explained considering that the system is under periodic boundary condition, thus when the wave packet reaches the limits of the chain it bounces back bringing a negative contribution to the spreading velocity. In fact, from fig. (5.2) one can see that the reflection of the wave packet starts for $t \approx 9$, and at the same time the spreading velocity in fig. (5.3) starts to decrease.
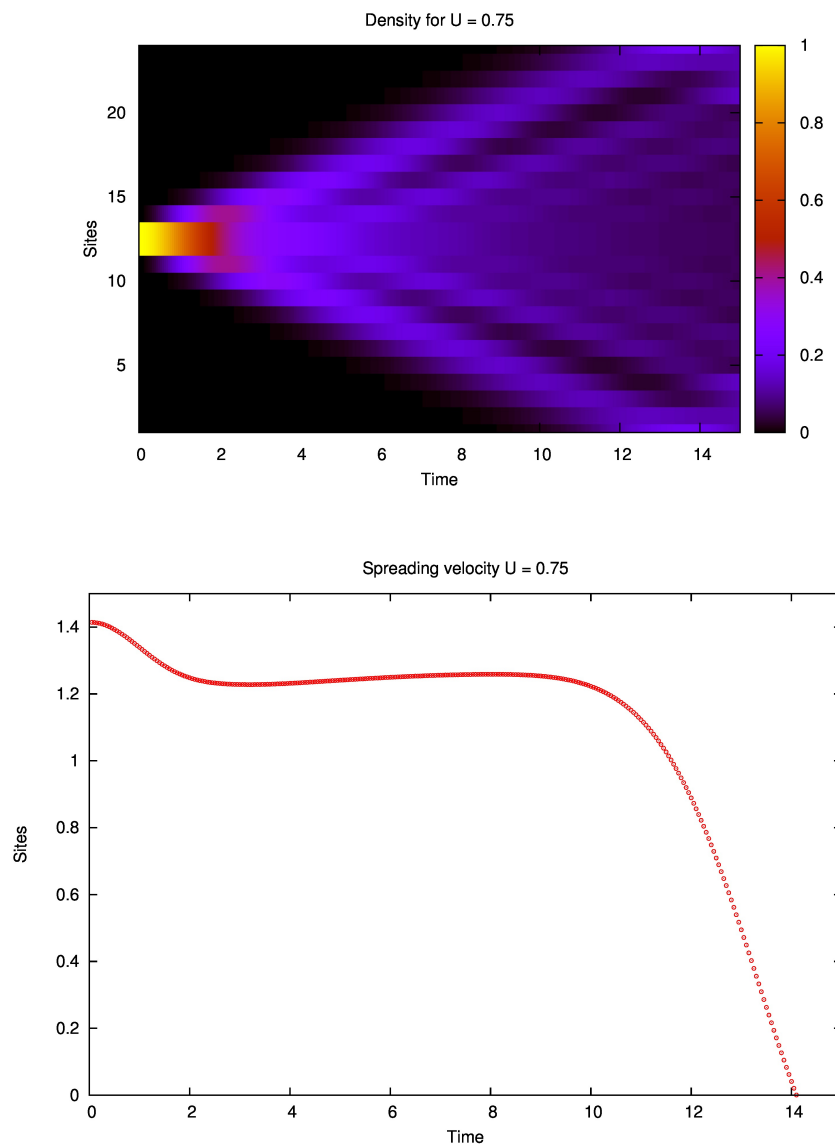
Interacting case with $U = 0.25$, $U = 0.75$ and $U = 1.00$
For different values of U the evolution shows the effects of the interaction.

In the following we will report for brevity only the results for $U > 0$, for negative values of U the evolution turns to be exactly the same.
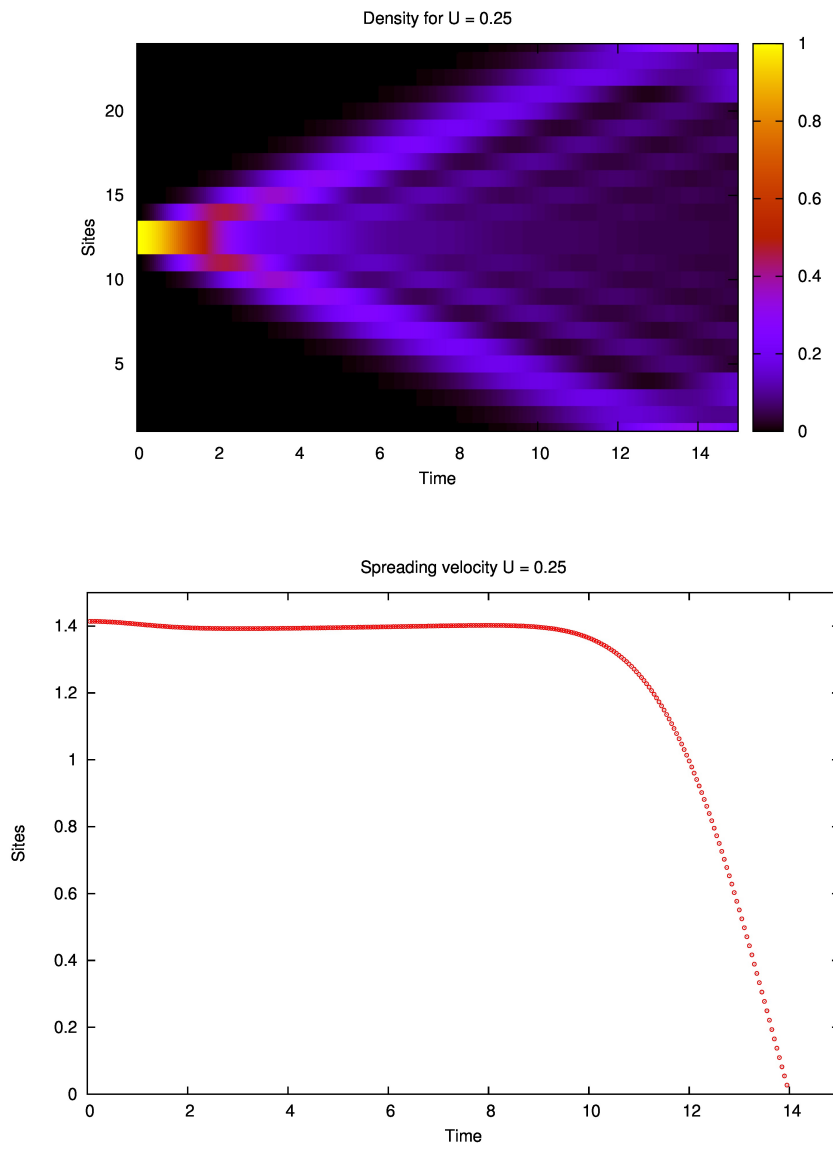
Figure 5.4: Density profile and spreading velocity of the system evolving with $U = 0.25$.

Figure 5.5: Density profile and spreading velocity of the system evolving with $U = 0.75$.
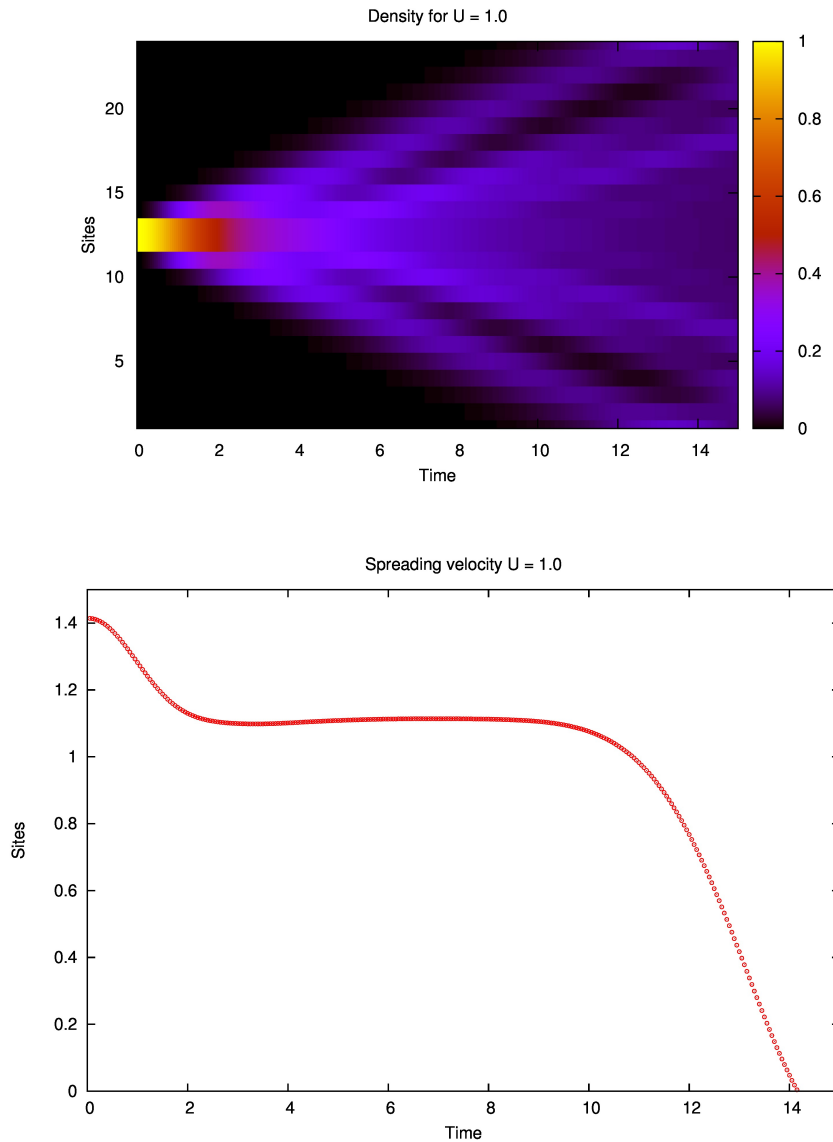
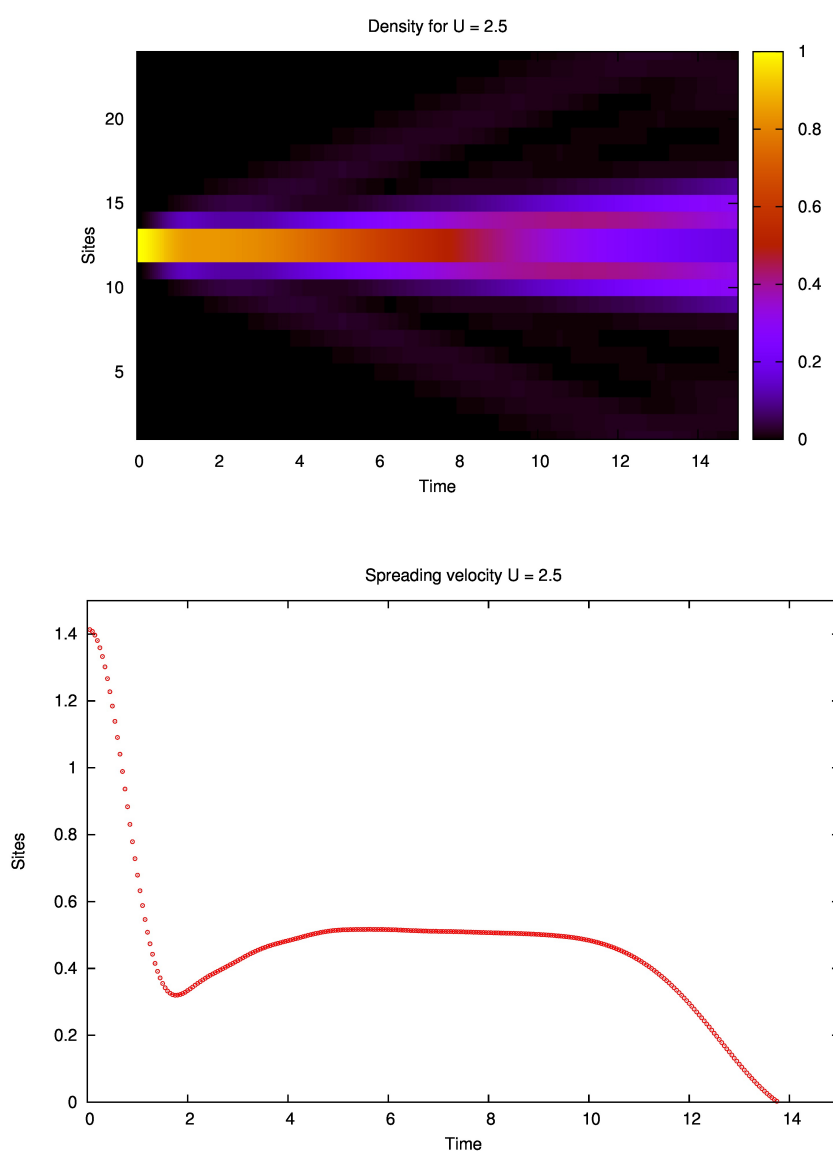**Figure 5.6**: Density profile and spreading velocity of the system evolving with $U = 1.0$.

Evaluating the graphs in figs. (5.4,5.5,5.6) one can see that during intial instant of the evolution, the system stay focused on the central sites of the chain but in a short time the scattering caracther prevail and the wave packet spreads along all the chain. However, from the graphs of the spreading speed in figs (5.4,5.5,5.6) it turns out that this spreading is realized with a lower speed than the free case.

This could be explained considering the presence of the bound states which

tend to constrain the wave packet to stay bounded to the central sites of the chain.

Interacting case with $U = 2.5$ and $U = 4.0$
For higher values of U the presence of bound states is more and more evident, we present here the results for only two intermediate values of U:

Figure 5.7: Density profile and spreading velocity of the system evolving with $U = 2.5$.
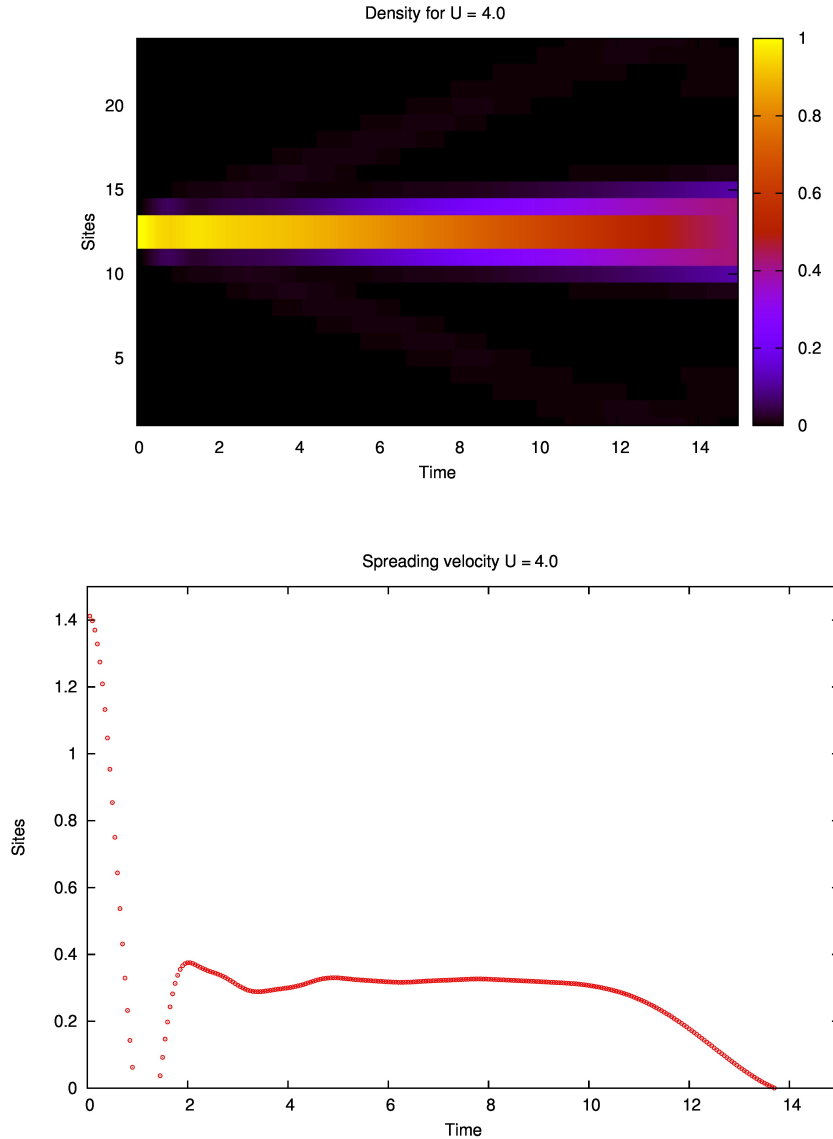
Figure 5.8: Density profile and spreading velocity of the system evolving with $U = 4.0$.

Examining the graphs in figs. (5.7, 5.8) one can see that the "spreading behaviour" is almost suppressed and the wave packet is very focused around the central sites of the chain.

Something peculiar cames from the graphs of the spreading velocity. The spreading velocity starts as expected from $v_{scatt} = \sqrt{2}$ but it decreases rapidly to a lower value and increases again reaching a sort of constant value.

The decreasing and increasing stage could be caused by the fact that the

"spreading" and "bounded" component in the wave packet start together, the former has velocity $v_{spread} = \sqrt{2}$ the latter tends to stay on the central sites so $v_{bound} \ll v_{spread}$.

At initial time the "spreading wave" is contained on central sites together with the "bounded wave", in this case the density of the "spreading wave" do not contributes to the evaluation of the spreading velocity so its value will fall rapidly toward v_{bound}. As soon as the "spreading wave" is able to reach other chain sites its contribute to the spreading velocity becomes appreciable, the spreading velocity increases again toward a value (the plateau in the spreading velocity graphs) that could be considered its asymptotic value.

Spreading velocity data for $t > 9$ are not to be considered because they are influenced by the reflection of the wave packet on the chain boundaries.

It is almost against the intuition that two particles with a repulsive next-neighbour interaction ($U > 0$) tends more and more to stay on adjacent sites as U is increased. Intuitively the repulsive interaction should force the particles to stay as much distant is possible.

Evaluating the asymptotic velocity one can find another surprisingly result, the asymptotic velocity decrease as U increase (fig. (5.9)). Again, despite the repulsive interaction, the particles prefer to stay bounded.
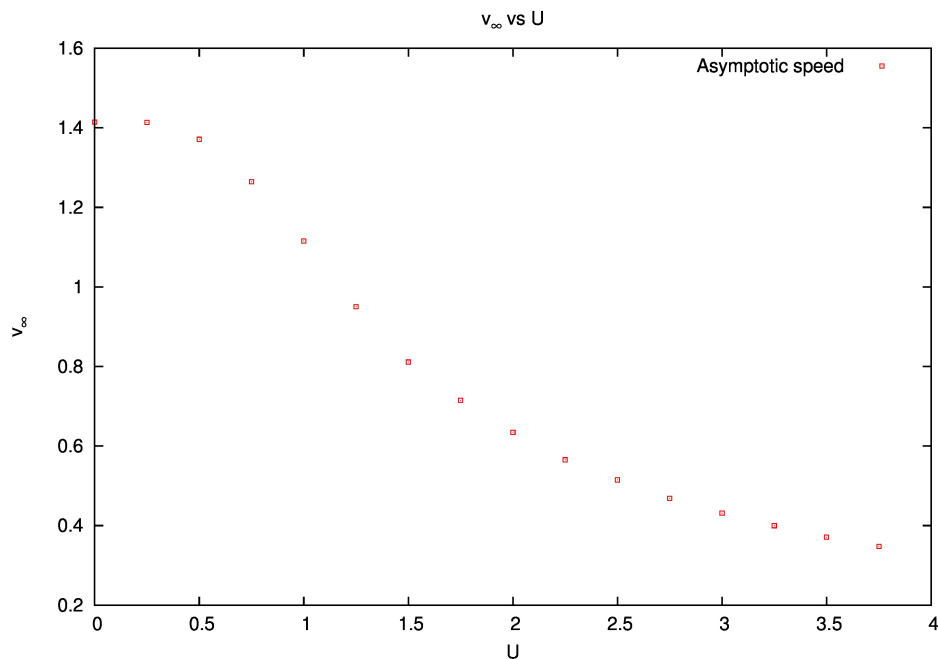
Figure 5.9: Asymptotic velocity v_∞ vs U.

This counterintuitive behaviour has been pointed out also in [4] and [5] respectively for the spin $\frac{1}{2}$ XXZ model and interacting bosons model.
For the interacting bosons model the authors conclude showing that the dynamics is strongly influenced by the presence of bound states. They are able to evaluate the quantity $P^B = \sum_\alpha \langle \Psi_0 | \Phi_\alpha^B \rangle$ which is the total projection of the initial state ($|\Psi_0\rangle$) over the bound state of the system ($|\Phi_\alpha^B\rangle$) for every value of U. It turns out that the asymptotic velocity decrease as $P^B(U)$ increase.

It could be interestingly to give a qualitative explaination of the role of bound states also in the dynamics of the SF model and spin $\frac{1}{2}$ XXZ model in terms of the quantity $P^B(U)$. Some information about the role of the bound states could be done extracted from the evaluation of the adjacent occupation defined as the quantity $\langle n_i n_{i+1} \rangle$ during the evolution of the system.
Moreover, it could be interestingly to study the dynamics of this system starting from a different initial state, perhaps an entangled state rather a pure state, and to extend this study to the case of more than two particles from both the analytical and the numerical sides.

Appendices

Appendix 1 - CBA on a system of $N = 2$ fermionic particles

Let us consider the following hamiltonian:

$$H = -\frac{t}{2}\sum_{i=1}^{L}\left(c_i^+ c_{i+1} + c_{i+1}^+ c_i\right) + U\sum_{i=1}^{L}(n_i - \frac{1}{2})(n_{i+1} - \frac{1}{2}) + \mu\sum_{i=1}^{L}(n_i - \frac{1}{2}) \quad (6)$$

The states we will consider are two-particles fermionic states of the form:

$$|\phi\rangle = \sum_{j,k=1}^{L} \phi_{j,k} c_j^+ c_k^+ |0\rangle = \sum_{j,k=1}^{L} \phi_{j,k}|j,k\rangle \quad (7)$$

With $\phi_{j,k}$ coefficient to be determined. Considering the fermionic property of the states, we must request that those coefficient are antisimmetric and that they obey to the Pauli's exclusion principle. So:

$$\phi_{j,k} = -\phi_{k,j} \text{ and } \phi_{j,j} = 0 \quad (8)$$

From the Schroedinger equation, one obtain:

$$-\frac{t}{2}\sum_{i=1}^{L}\sum_{j,k=1}^{L}\left(c_i^+ c_{i+1} + c_{i+1}^+ c_i\right)\phi_{j,k}|j,k\rangle +$$

$$+U\sum_{i=1}^{L}\sum_{j,k=1}^{L}(n_i - \frac{1}{2})(n_{i+1} - \frac{1}{2})\phi_{j,k}|j,k\rangle +$$

$$+\mu\sum_{i=1}^{L}\sum_{j,k=1}^{L}(n_i - \frac{1}{2})\phi_{j,k}|j,k\rangle =$$

$$= E\sum_{j,k=1}^{L}\phi_{j,k}|j,k\rangle \quad (9)$$

$$-\frac{t}{2} \sum_{i=1}^{L} \sum_{j,k=1}^{L} \phi_{j,k} c_i^+ c_{i+1} |j,k\rangle - \frac{t}{2} \sum_{i=1}^{L} \sum_{j,k=1}^{L} \phi_{j,k} c_{i+1}^+ c_i |j,k\rangle +$$

$$+ U \sum_{i=1}^{L} \sum_{j,k=1}^{L} n_i n_{i+1} \phi_{j,k} |j,k\rangle - U \sum_{i=1}^{L} \sum_{j,k=1}^{L} n_i \phi_{j,k} |j,k\rangle + \frac{L}{4} U \sum_{j,k=1}^{L} \phi_{j,k} |j,k\rangle +$$

$$+ \mu \sum_{i=1}^{L} \sum_{j,k=1}^{L} n_i \phi_{j,k} |j,k\rangle - \frac{L}{2} \mu \sum_{j,k=1}^{L} \phi_{j,k} |j,k\rangle =$$

$$= E \sum_{j,k=1}^{L} \phi_{j,k} |j,k\rangle \tag{10}$$

$$-\frac{t}{2} \sum_{i=1}^{L} \sum_{j,k=1}^{L} \phi_{j,k} |j-1,k\rangle + \frac{t}{2} \sum_{i=1}^{L} \sum_{j,k=1}^{L} \phi_{j,k} |j,k-1\rangle +$$

$$-\frac{t}{2} \sum_{i=1}^{L} \sum_{j,k=1}^{L} \phi_{j,k} |j+1,k\rangle + \frac{t}{2} \sum_{i=1}^{L} \sum_{j,k=1}^{L} \phi_{j,k} |j,k+1\rangle +$$

$$+ U \sum_{j,k=1}^{L} (\delta_{j,k+1} + \delta_{k,j+1}) \phi_{j,k} |j,k\rangle +$$

$$+ (2\mu - 2U + \frac{L}{4} U - \frac{L}{2} \mu) \sum_{j,k=1}^{L} \phi_{j,k} |j,k\rangle =$$

$$= E \sum_{j,k=1}^{L} \phi_{j,k} |j,k\rangle \tag{11}$$

And, finally:

$$\sum_{j=1}^{L} \sum_{k=1}^{L} [-\frac{t}{2} (\phi_{j+1,k} + \phi_{j,k+1} + \phi_{j-1,k} + \phi_{j,k-1}) + \tag{12}$$

$$+ \phi_{j,k} (U\delta_{j,k+1} + U\delta_{k,j+1} - 2U + 2\mu + \frac{UL}{4} - \frac{\mu L}{2} - E)] |j,k\rangle = 0 \tag{13}$$

We can do a Bethe ansatz on the coefficients $\phi_{j,k}$, so:

$$\phi_{j,k} = [Ae^{i(p_1 j + p_2 k)} + Be^{i(p_1 k + p_2 j)}] \theta(j-k) - [Ae^{i(p_1 k + p_2 j)} + Be^{i(p_1 j + p_2 k)}] \theta(k-j) \tag{14}$$

The minus sign take account of the antisimmetric property, it is easy to verify that:

$$\phi_{j,k} = -\phi_{k,j} \tag{15}$$

Furthermore, the functions $\theta(j-k)$ and $\theta(k-j)$ are the step function (or Heaviside's Theta) which let us discriminate between the cases $j > k$ or $k > j$. Note the strict disequality, this is given to the Pauli's exclusion principle which impose $j \neq k$. This condition is automatically implemented in the ansatz in fact, as previously said, the quantity $\phi_{j,j}$ vanish. Now, let us study the eq.(12) when $j > k + 1$:

$$-\frac{t}{2}(\phi_{j+1,k}+\phi_{j,k+1}+\phi_{j-1,k}+\phi_{j,k-1})+\phi_{j,k}(2\mu-2U+\frac{UL}{4}-\frac{\mu L}{2}-E) = 0 \quad (16)$$

Define $F_{j,k}^{j>k+1} = (\phi_{j+1,k} + \phi_{j,k+1} + \phi_{j-1,k} + \phi_{j,k-1})$:

$$(\phi_{j+1,k} + \phi_{j,k+1} + \phi_{j-1,k} + \phi_{j,k-1}) =$$

$$= [Ae^{i(p_1 j+p_2 k+p_1)} + Be^{i(p_1 k+p_2 j+p_2)}]+$$
$$+[Ae^{i(p_1 j+p_2 k+p_2)} + Be^{i(p_1 k+p_2 j+p_1)}]+$$
$$+[Ae^{i(p_1 j+p_2 k-p_1)} + Be^{i(p_1 k+p_2 j-p_2)}]+$$
$$+[Ae^{i(p_1 j+p_2 k-p_2)} + Be^{i(p_1 k+p_2 j-p_1)}] =$$

$$= (Ae^{i(p_1 j+p_2 k)} + Be^{i(p_1 k+p_2 j)})(e^{ip_1} + e^{-ip_1} + e^{ip_2} + e^{-ip_2}) =$$

$$= 4(Ae^{i(p_1 j+p_2 k)} + Be^{i(p_1 k+p_2 j)})(\cos(p_1) + \cos(p_2)) \quad (17)$$

$$F_{j,k}^{j<k+1} = 4\phi_{j,k}(\cos(p_1) + \cos(p_2)) \quad (18)$$

So:

$$E^{j>k+1} = -2t(\cos(p_1) + \cos(p_2)) + 2\mu - 2U + \frac{UL}{4} - \frac{\mu L}{2} \quad (19)$$

Considering the case $k > j + 1$ we have to proceed exactly in the same way. In this case for $F_{j,k}^{k>j+1}$ and $E^{k>j+1}$ one obtain:

$$F_{j,k}^{k>j+1} = 4\phi_{j,k}(\cos(p_1) + \cos(p_2)) \quad (20)$$

$$E^{k>j+1} = -2t(\cos(p_1) + \cos(p_2)) + 2\mu - 2U + \frac{UL}{4} - \frac{\mu L}{2} \quad (21)$$

The results are the same, so:

$$E = E^{k>j+1} = E^{j>k+1} = -2t(\cos(p_1) + \cos(p_2)) + 2\mu - 2U + \frac{UL}{4} - \frac{\mu L}{2} \quad (22)$$

Let us define

$$E_0^{(2)} = +2\mu - 2U + \frac{UL}{4} - \frac{\mu L}{2}$$

Consider now the cases $j = k + 1$ and $k = j + 1$. When $j = k + 1$ the eq.(12) take the form:

$$-\frac{t}{2}(\phi_{k+2,k} + \phi_{k+1,k-1}) + U\phi_{k+1,k} + (E_0^{(2)} - E)\phi_{k+1,k} = 0 \qquad (23)$$

Subtituing the expression for E from the eq.(22):

$$-\frac{t}{2}(\phi_{k+2,k}+\phi_{k+1,k-1})+U\phi_{k+1,k}+(E_0^{(2)}+2t\left(\cos(p_1)+\cos(p_2)\right)-E_0^{(2)})\phi_{k+1,k} = 0$$
$$(24)$$

so:

$$-\frac{t}{2}(\phi_{k+2,k} + \phi_{k+1,k-1}) + U\phi_{k+1,k} + 2t\left(\cos(p_1) + \cos(p_2)\right)\phi_{k+1,k} = 0 \quad (25)$$

But:

$$2t\left(\cos(p_1) + \cos(p_2)\right)\phi_{k+1,k} =$$

$$= \frac{t}{2}(e^{ip_1} + e^{-ip_1} + e^{ip_2} + e^{-ip_2})\phi_{k+1,k} =$$

$$= \frac{t}{2}(e^{ip_1} + e^{-ip_1} + e^{ip_2} + e^{-ip_2})[Ae^{i(p_1k+p_2k+p_1)} + Be^{i(p_1k+p_2k+p_2)}] =$$

$$= \frac{t}{2}\left[Ae^{i(p_1k+p_2k)}\left(e^{i2p_1} + 1 + e^{i(p_2+p_1)} + e^{-i(p_2-p_1)}\right)\right] +$$
$$+ \frac{t}{2}\left[Be^{i(p_1k+p_2k)}\left(e^{i(p_1+p_2)} + e^{-i(p_1-p_2)} + e^{i2p_2} + 1\right)\right] \qquad (26)$$

So:

$$-\frac{t}{2}(Ae^{i(p_1k+p_2k+2p_1)} + Be^{i(p_1k+p_2k+2p_2)}+$$
$$+Ae^{i(p_1k+p_2k+p_1-p_2)} + Be^{i(p_1k+p_2k+p_2-p_1)})+$$
$$+U[Ae^{i(p_1k+p_2k+p_1)} + Be^{i(p_1k+p_2k+p_2)}]+$$
$$+\frac{t}{2}[Ae^{i(p_1k+p_2k)}\left(e^{i2p_1} + 1 + e^{i(p_2+p_1)} + e^{-i(p_2-p_1)}\right)+$$
$$+Be^{i(p_1k+p_2k)}\left(e^{i(p_1+p_2)} + e^{-i(p_1-p_2)} + e^{i2p_2} + 1\right)] = 0 \qquad (27)$$

$$\frac{t}{2}(Ae^{i(p_1k+p_2k)} + Be^{i(p_1k+p_2k)})(1 + e^{i(p_2+p_1)})+$$
$$+U(Ae^{i(p_1k+p_2k)}e^{ip_1} + Be^{i(p_1k+p_2k)}e^{ip_2}) = 0 \qquad (28)$$

Finally, one can write:

$$\frac{A}{B} = -\frac{1 + e^{i(p_2+p_1)} + \frac{2U}{t}e^{ip_2}}{1 + e^{i(p_2+p_1)} + \frac{2U}{t}e^{ip_1}} \tag{29}$$

In the same way, for $x = -1$, we obtain from eq.(12):

$$-\frac{t}{2}(\phi_{j,j+2} + \phi_{j-1,j+1}) + \phi_{j,j+1}(U + 2U + \mu + \frac{LU}{4} - E) = 0 \tag{30}$$

Which lead to an expression for $\frac{B}{A}$ similar to eq.(29):

$$\frac{A}{B} = -\frac{1 + e^{i(p_2+p_1)} + \frac{2U}{t}e^{ip_1}}{1 + e^{i(p_2+p_1)} + \frac{2U}{t}e^{ip_2}} \tag{31}$$

It can be shown that, in both cases, the quantity $\frac{A}{B}$ is equivalent to a phase factor:

$$\frac{A}{B} = e^{i\theta} \tag{32}$$

Acknowledgement

Bibliography

[1] A. Avella, F. Mancini, Eur. Phys. J. B 41, 149 (2004)

[2] H. Bethe, Z. Phys. 71, 205 (1931)

[3] J.C. Bonner and M.E. Fisher, Phys. Rev. 135, A640 (1964)

[4] L. Bonnes, F. H. L. Essler, A. M. Läuchli, arXiv:1404.4062

[5] C. Degli Esposti Boschi, E. Ercolessi, L. Ferrari, P. Naldesi, F. Ortolani, L. Taddia, Arxiv_1407.2105 (accepted for pubblication on PRA) (2014)

[6] P. F. Carcia, A. D. Meinhaldt and A. Suna, Appl. Phys. Lett. 47, 178 (1985)

[7] E. Ercolessi, P. Pieri, M.Roncaglia, Phys. Lett. A 233, 451 (1997)

[8] R.P. Feynman, "Lectures on Physics", Addison Wesley Longman (January 1, 1970)

[9] M. K. Fung, J. Math. Phys. 22, 2017 (1981)

[10] J. Gaite, quant-ph/0301120 (2003)

[11] *P. S. Goldbaum, arXiv:cond-mat/0403736 (2004)

[12] J. Hubbard, Proc. Roy. Soc. A 276 238 (1963)

[13] S. Ikeda, K. Miura, H. Yamamoto, K. Mizunuma, H. D. Gan, M. Endo, S. Kanai, J. Hayakawa, F. Matsukura & H. Ohno, Nature Materials 9, 721–724 (2010)

[14] P. Jordan and E. Wigner, Z. Phys. 47, 631 (1928)

[15] M. Karbach and G. Müller, Comp. in Phys. 11, 36 (1997)

[16] T. Kinoshita, T. Wenger, and D. S. Weiss, Nature 440, 900 (2006)

[17] C. Kollath, "The adaptive time-dependent density-matrix renormalization-group method: development and applications." Master's degree. thesis. Rheinisch-Westfalischen Technischen Hochschule: Germany (2005)

[18] J. I. Latorre, E. Rico, and G. Vidal, Quant. Inf. Comp. 4, 48 (2004)

[19] O. Legeza, and G. F'ath, Phys. Rev. B 53, 14349 (1996)

[20] E. Lieb, XI Int. Cong. MP, Int. Press 392-412 (1995)

[21] R. Orbach, Phys. Rev. 112, 309 (1958)

[22] T. J. Osborne, and M. A. Nielsen, Quant. Inf. Proc. 1, 45 (2002)

[23] U. Schollwoeck, Rev. Mod. Phys, (2005)

[24] B. Sutherland, Phys. Rev. Lett. 20, no. 3, 98 (1968)

[25] M. Takahashi, "Thermodynamics of One-Dimensional Solvable Models", Cambridge University Press (1999)

[26] L. R. Walker, Phys. Rev. 116, 1089 (1959)

[27] S. R. White, Phys. Rev. Lett., 69:2863, (1992)

[28] S. R. White, Phys. Rev. B, 48:10345, (1993)

[29] S. R.White and D. Huse, Phys. Rev. B 48, 3844 (1993)

[30] C.N. Yang and C.P. Yang, Phys. Rev. 147, 303 (1996)

[31] C.N. Yang and C.P. Yang, Phys. Rev. 150, 321 (1996)

[32] C.N. Yang and C.P. Yang, Phys. Rev. 150, 327 (1996)

[33] C.N. Yang and C.P. Yang, Phys. Rev. 151, 258 (1996)

[34] C. N. Yang, Phys. Rev. Lett. 19, no. 23, 1312 (1967)